

# Studying Cosmic Magnetism in the Nearby Universe with LOFAR

## LOFAR Key Science Project Project Plan

P. Alexander<sup>1</sup>, J. M. Anderson<sup>2</sup>, R. Beck<sup>2</sup>, D. J. Bomans<sup>3</sup>, M. Brentjens<sup>4,5</sup>,  
A. G. de Bruyn<sup>4,5</sup>, K. T. Chyży<sup>6</sup>, R.-J. Dettmar<sup>3</sup>, S. Duscha<sup>7</sup>, J. Eislöffel<sup>8</sup>,  
T. A. Enßlin<sup>7</sup>, K. Ferrière<sup>9</sup>, J. Geisbüsch<sup>1</sup>, M. Haverkorn<sup>4,10</sup>, G. Heald<sup>4</sup>, M. Jamrozy<sup>6</sup>,  
U. Klein<sup>11</sup>, A. Noutsos<sup>2</sup>, P. Papaderos<sup>11</sup>, W. Reich<sup>2</sup>, A. Scaife<sup>1</sup>, M. Soida<sup>6</sup>, M. Urbanik<sup>6</sup>

<sup>1</sup> Cavendish Laboratory Cambridge, UK

<sup>2</sup> Max-Planck-Institut für Radioastronomie Bonn, Germany

<sup>3</sup> Astronomisches Institut der Ruhr-Universität Bochum, Germany

<sup>4</sup> ASTRON Dwingeloo, The Netherlands

<sup>5</sup> Kapteyn Institute Groningen, The Netherlands

<sup>6</sup> Astronomical Observatory Kraków, Poland

<sup>7</sup> Max-Planck-Institut für Astrophysik Garching, Germany

<sup>8</sup> Thüringer Landessternwarte Tautenburg, Germany

<sup>9</sup> Observatoire Midi-Pyrénées, France

<sup>10</sup> Leiden Observatory, The Netherlands

<sup>11</sup> Argelander-Institut für Astronomie der Universität Bonn, Germany

Version 2.6  
2010 Jan. 10

# Contents

1. Summary	3
2. Scientific motivation	3
2.1 Low-frequency synchrotron emission	5
2.2 Polarization and Faraday rotation at low frequencies	7
2.3 Rotation Measure Synthesis	8
3. Milky Way	11
3.1 Surveys	11
3.2 Faraday screens	14
3.3 The local interstellar cloud and the local bubble	14
3.4 The Galactic halo and disk-halo interface	15
3.5 Galactic turbulence	15
3.6 Pointed Galactic observations	16
3.7 The large-scale Galactic magnetic field	16
4. Magnetic fields in spiral galaxies	17
4.1 Galactic dynamos	17
4.2 Outer disks and halos of spiral galaxies	19
5. Perturbed galaxies and galaxy groups	24
5.1 Tidal interactions and IGM ram pressure	24
5.2 Galaxy groups	29
6. Dwarf galaxies	31
7. Giant radio galaxies	34
8. Stellar and AGN jets	36
9. Intergalactic magnetic fields	38
10. Observing program	41
10.1 Deep mapping and RM grids	41
10.2 Polarization calibration	46
10.3 Ionospheric calibration	46
10.4 Relations to the other LOFAR Key Science Projects	47
10.5 Theoretical investigations	47
References	48

# 1 Summary

The international LOFAR Key Science Project on *Cosmic Magnetism in the Nearby Universe* (MKSP) plans to study magnetic fields in the Milky Way and nearby galaxies by observing total and polarized radio synchrotron emission at low frequencies. Polarimetry with LOFAR will allow the investigation of the so far unexplored domain of very small Faraday rotation measures and hence weak magnetic field strengths. Through deep observations of the diffuse total and polarized emission and the Faraday rotation towards polarized background sources, the Project will investigate the dynamical importance of magnetic fields in the disks and halos of nearby galaxies, dwarf galaxies and intergalactic filaments in compact galaxy groups. For the first time we might detect magnetic fields and tenuous warm gas expelled from the star-forming regions in external galaxies, extending far into the intergalactic medium. The technique of *RM Synthesis* will allow the investigation of the 3-D structure of magnetic fields in the local Milky Way and in nearby galaxies. As a collaboration, similar studies of radio galaxies and galaxy clusters are planned by the LOFAR *Surveys* Key Science Project.

We plan to use LOFAR to detect the radio emission in galactic gaseous features at the distance of tens of kpc from the star-forming disks, like extended gaseous halos of spiral and dwarf irregulars, or tails of interacting and stripped spirals. It is essential to know the magnetic pressure and energy density in such structures to determine properly the physical conditions in the gas. Very low frequencies ( $\nu < 200$  MHz) are required, as the CR electrons emitting in this spectral domain live and travel away ten times farther than those visible at centimeter wavelengths. Polarization studies are crucial here: both the magnetic pressure and CR propagation speed depends on the magnetic field geometry. The magnetic diagnostic of the gas flows will also be possible while the Faraday rotation will help to distinguish between compressed/sheared random fields and regular ones. With a low ionized gas density and weak magnetic fields the expected RM amounts to few  $\text{rad/m}^2$ . To obtain small RM errors, a wide frequency span is required.

Faraday rotation from pulsars will be measured in collaboration with the LOFAR *Transients* Key Science Project and will yield a detailed picture of the regular magnetic fields near the sun. Pulsars are also ideal polarization calibrators. As another class of polarization calibrators, giant radio galaxies will be observed. Searches for synchrotron emission from jets of young stars, including linear and circular polarization, are also planned.

Strong support for the work of the Project comes from the German Research Foundation (DFG) which is funding a Research Group of 10 PhD students and 2 postdocs for the period 2010–13, lead by 10 German scientists from 8 institutes on the topic “Magnetisation of Interstellar and Intergalactic Media: The Prospects of Low-Frequency Radio Observations”.

## 2 Scientific motivation

Understanding the Universe is impossible without understanding magnetic fields. Magnetic fields are present in almost every place in the Universe. Most of the luminous matter is tightly coupled to magnetic fields. Magnetic fields are the dominant agent in radio galaxies. Large-scale fields intersperse the gas in star-forming galaxies and in galaxy clusters, and they contribute to the nonlinear interplay of turbulent motions in the intracluster and interstellar medium. The magnetic energy content affects the evolution of galaxies, galaxy clusters and the gaseous halos of radio galaxies, it contributes significantly to the total pressure of interstellar gas, is essential for the onset of star formation and controls the density and distribution of cosmic rays in the interstellar medium (ISM). In spite of their importance, the evolution,

structure and origin of magnetic fields are still open problems in fundamental physics and astrophysics.

Most of what we know about astrophysical magnetic fields has been detected via radio astronomical observations, as extragalactic radio emission is mainly synchrotron radiation by relativistic leptons. The observed intensity of *synchrotron emission* is related to the total field strength, while its polarization yields the orientation of the ordered field in the plane of the sky and also gives the field's degree of ordering. Moreover, *Faraday rotation* provides information on the component of the regular field along the line of sight and its direction. During the last 30 years, radio continuum observations of the Milky Way, nearby galaxies and galaxy clusters have enormously increased our knowledge about the structure and strength of interstellar magnetic fields in galaxies and intergalactic magnetic fields in clusters.

Important information on magnetic fields in galaxies comes from the relation between the total radio and far-infrared flux densities of galaxies and also between the radio and far-infrared intensities within galaxy disks. This very tight correlation is very robust and one of the most puzzling relations in extragalactic research. It holds across a remarkable variety of galaxies, to include normal disk galaxies, dwarf galaxies and starburst galaxies. It extends over five orders of magnitude, and down to smallest scales of about 100 pc. As the radio flux of galaxies is dominated by synchrotron emission, the correlation strongly suggests that the processes of star formation and magnetic field amplification are closely connected.

The radio–far-infrared correlation holds also for distant galaxies, to at least redshifts of 3. Hence magnetic fields existed already in young galaxies with strengths similar to, or larger than, those in present-day galaxies. As the magnetic energy density in nearby galaxies is comparable to that of the turbulent gas motions and much larger than the thermal energy density, the evolution of galaxies may have been affected by their magnetic fields.

The large-scale field structure in the Milky Way and almost all nearby galaxies was found to have a spiral structure, with pitch angles similar to those of the optical spiral arms. However, spiral fields were also detected in galaxies without any optical spiral structure. Faraday rotation revealed large-scale coherence (same direction) of the spiral fields in many galaxies. This indicates the action of alpha-omega *dynamos* in galaxies, where shearing motions driven by differential rotation act together with the Coriolis force of turbulent gas motions to amplify the weak seed fields exponentially and thus generate large-scale fields. The estimated growth time for large-scale fields is a few Gyr, but the ordering timescale until full coherence of the large-scale regular field is longer and may exceed the galaxy age for the largest galaxies.

The physics of the galactic dynamo is far from being understood. It still seems possible that primordial fields from a galaxy's early days are significantly amplified and stretched by compressing and shearing gas flows in a non-axisymmetric gravitational potential, and a dynamo may only be needed to obtain the large-scale coherence. MHD models including the volume of a galaxy are needed, but present-day models are limited by the grid size to small volumes that do not encompass spiral arms, bars and halos.

A major obstacle to dynamo action is the preservation of total helicity which leads to a quenching of dynamo action. Small-scale field helicity from galactic disks has to be removed. There is indeed increasing evidence that galaxies are open systems. Hot gas and cosmic rays from star-forming regions can drive outflows that are continuously expelling magnetic energy and small-scale helicity into the intergalactic medium. Outflows are indispensable for the continuous build-up of large-scale helicity by the dynamo.

Cosmic-ray driven dynamos may operate in differentially rotating galaxies that still form stars and produce supernovae. Supernova shock waves are the sources of high energy cosmic rays which are tightly coupled to the galactic magnetic fields. Cosmic-ray pressure is supposed to be of the same order as any dynamical pressure in the interstellar medium and thus they

may be involved in the dynamo cycle in which pressure forces and kinetic gas energy density is transformed into magnetic energy density. The action of a cosmic-ray dynamo is then directly related to the star formation rate and star formation history of a galaxy. Furthermore, such cosmic-ray driven dynamo models have the potential to explain the intriguing radio–far-infrared correlation.

Cosmic magnetic fields recently attracted special attention of the AUGER team who claimed that some of the arrival directions of detected ultrahigh-energy cosmic rays (UHECRs,  $> 10^{19}$  eV) are coincident with positions of known nearby active galaxies. However, the interpretation is hampered by our lack of knowledge of the structure and strength of the magnetic field in the halo of our Milky Way and beyond. Only measurements of the Faraday rotation towards a large number of background sources can bring progress, and LOFAR is specially suited to measure low Faraday rotation in galactic halos.

From cosmological models of structure formation, the intergalactic space is probably permeated by magnetic filaments. Galactic winds and the frequent interactions between galaxies may further increase the magnetization of the intergalactic medium. The detection of magnetic fields in intergalactic filaments and observational tests of the connection between disk fields and intergalactic fields have to await more sensitive radio telescopes like LOFAR.

## 2.1 Low-frequency synchrotron emission

Low-frequency radio emission from the Milky Way and galaxies out to redshifts of about 3 is almost purely nonthermal. Total synchrotron intensity  $I$  and its linear polarization can be used to measure the strengths of the total magnetic field and its regular component, assuming equipartition between the energy densities of magnetic fields and cosmic rays, and assuming a number density ratio of proton to electrons of 100 (see Beck & Krause 2005 for a discussion). With the VLA, intensities of  $I \simeq 20 \mu\text{Jy}$  per beam can be detected at 1.4, 4.8 and 8.6 GHz within 12 hours of observing time. With the WSRT, a similar sensitivity can be reached at 1.2–1.8 GHz. Diffuse emission from cosmic-ray electrons in a  $5 \mu\text{G}$  equipartition field (perpendicular to the line of sight) can be detected in galaxies ( $\simeq 1$  kpc pathlength) or a  $1 \mu\text{G}$  equipartition field in clusters ( $\simeq 1$  Mpc pathlength) with a telescope beam of about  $15''$  diameter. The Effelsberg 100-m telescope can typically measure polarized intensities of  $\simeq 200 \mu\text{Jy}$  per beam at 4.8 GHz ( $2.4'$  beam) and  $\simeq 100 \mu\text{Jy}$  at 8.3 GHz ( $82''$  beam), if the source extent is moderate so that a large number of coverages can be obtained within reasonable observing time. This corresponds to an equipartition strength of the large-scale regular field of  $\simeq 2 \mu\text{G}$  in galaxies and  $\simeq 0.4 \mu\text{G}$  in clusters. In principle, still deeper observations of large-scale regular fields are possible as there is little confusion in polarization due to background sources (but possibly due to polarized emission in the Milky Way foreground). For total field strengths there is a detection limit due to confusion of total intensity in the large Effelsberg beam, about  $5 \mu\text{G}$  for galaxies and about  $1 \mu\text{G}$  for clusters. These sensitivities are sufficient to map magnetic fields in the Milky Way, in galaxy disks, in bright halos and bright clusters. However, magnetic fields may occur in much larger volumes of the Universe where no cosmic-ray electrons of sufficient energy exist to illuminate them.

Cosmic-ray electrons can be generated in shocks and by pion decay of cosmic-ray protons. In clusters, cosmic-rays can also be injected by AGN activity (quasars, radio galaxies, etc.), or by galactic winds from strongly star-forming galaxies, or they can be accelerated from the thermal pool by large-scale shocks during the cluster dynamical history and further re-accelerated by shocks and turbulence in the intracluster medium.

Generation of cosmic-ray electrons in shocks or by pion decay generates steep electron energy spectra, giving rise to synchrotron radio spectra with a negative power-law slope. Emission from electrons in weak magnetic fields can thus be observed at low frequencies.

The synchrotron intensity (per constant beam) is proportional to  $\nu^{-\alpha} B^{\alpha+1}$  (where  $\alpha$  is the synchrotron spectral index, defined as  $S \propto \nu^{-\alpha}$ ) for constant cosmic-ray density and to  $\nu^{-\alpha} B^{\alpha+3}$  for the equipartition case. The synchrotron brightness temperature of an extended source is proportional to  $\nu^{-(\alpha+2)} B^{\alpha+1}$  and  $\nu^{-(\alpha+2)} B^{\alpha+3}$ , respectively. For a fixed minimum detectable value of the brightness temperature, the minimum detectable field is proportional to  $\nu^{(\alpha+2)/(\alpha+1)}$  for constant cosmic-ray density and  $\nu^{(\alpha+2)/(\alpha+3)}$  for the equipartition case. Hence, observing at a  $10\times$  lower frequency (with the same telescope and the same sensitivity) allows us to detect  $\simeq 5\times$  weaker magnetic fields (assuming  $\alpha = 0.8$  and equipartition), but with  $10\times$  lower resolution. If the resolution and sensitivity are constant (e.g. by using a larger telescope configuration), the minimum detectable field varies with  $\nu^{\alpha/(\alpha+3)}$ , so that observing at a  $10\times$  lower frequency still allows us to detect  $\simeq 2\times$  weaker magnetic fields.

In star-forming regions, low-frequency radio emission can be reduced by thermal absorption or even disappear by synchrotron self-absorption in galactic nuclei. Regions of much lower thermal electron density, away from galaxy disks and active nuclei, maintain their steep emission spectrum and can become prominent at low frequencies, so that emission from relatively weak magnetic fields is observable.

The extent of synchrotron sources is limited by the propagation speed and the lifetime of primary electrons, which in turn is limited by synchrotron and inverse Compton (IC) losses:

$$t_{1/2} = 1.59 \cdot 10^9 \frac{B^{1/2}}{B^2 + B_{\text{CMB}}^2} \left[ \left( \frac{\nu}{\text{GHz}} \right) (1+z) \right]^{-1/2}, \quad (1)$$

where

$$B_{\text{CMB}} = 3.25 (1+z)^2 \mu\text{G} \quad (2)$$

is the equivalent magnetic field strength of the cosmic microwave background (CMB) at redshift  $z$ . This latter equation results from the similar dependencies of synchrotron and inverse Compton losses,

$$\dot{E}_{\text{syn}} \propto -u_{\text{mag}} E^2 \quad (3)$$

$$\dot{E}_{\text{IC}} \propto -u_{\text{rad}} E^2, \quad (4)$$

where  $u_{\text{mag}}$  is the magnetic energy density  $u_{\text{mag}} = B^2/8\pi$  and  $u_{\text{rad}}$  is the energy density of the radiation field (which for the perfect black-body CMB radiation is  $\propto T_{\text{CMB}}^4$ ).

The lifetime of electrons  $t_{\text{syn}}$  due to synchrotron losses increases with decreasing frequency and decreasing field strength ( $t_{\text{syn}} = 1.1 \cdot 10^9 \text{ yr } (\nu/\text{GHz})^{-0.5} (B/\mu\text{G})^{-1.5}$ ). In a  $5 \mu\text{G}$  field the lifetime of electrons emitting in the LOFAR bands is  $(2\text{--}5) \cdot 10^8 \text{ yr}$ . In magnetic fields weaker than  $3.25 \mu\text{G}$  ( $z+1$ )<sup>2</sup> the electron lifetime is limited by the inverse Compton effect on CMB photons. For pure inverse Compton loss ( $B \leq 1 \mu\text{G}$ ), the dependence of the lifetime of electrons (emitting at frequency  $\nu$ ) on field strength  $B$  has a reversed sign in the exponent ( $t_{\text{syn}} = 1.0 \cdot 10^8 \text{ yr } (\nu/\text{GHz})^{-0.5} (B/\mu\text{G})^{0.5}$ ), yielding a maximum lifetime of electrons for fields of about  $3 \mu\text{G}$  strength. (Note that in the disks of galaxies, especially starburst galaxies, the energy density of stellar photons may significantly exceed the CMB energy density, at least at low redshifts, so that the estimates of particle lifetimes and detectable magnetic fields are different.)

The extent of synchrotron-emitting sources is also determined by the propagation speed of cosmic-ray electrons. In turbulent magnetic fields, cosmic rays can stream with a speed equal to the Alfvén speed. In the disks of normal galaxies, the short lifetime of the electrons restricts their propagation length and hence their radio emission to about 1 kpc from their sources.

Low-frequency radio emission traces low-energy cosmic-ray electrons which suffer less from energy losses and can propagate further away from their sources into regions with weak

magnetic fields. Furthermore, the Alfvén speed is larger in the hot medium of galaxy halos or cluster halos.  $n_e \simeq 10^{-3} \text{ cm}^{-3}$  gives an Alfvén speed of  $\simeq 70 \text{ km/s } (B/\mu\text{G})$ . Streaming at this speed, an electron radiating at 50 MHz can propagate  $\simeq 330 \text{ kpc}/(B/\mu\text{G})^{0.5}$  during its lifetime for field strengths above  $B \geq 3 \mu\text{G}$  and about  $30 \text{ kpc } (B/\mu\text{G})^{1.5}$  for  $B \leq 3 \mu\text{G}$ . The maximum propagation length of about **200 kpc** is expected for field strengths around  $3 \mu\text{G}$ . The propagation length is even higher in regular magnetic fields. Galaxies are expected to be HUGE at low frequencies!

Finally, the widely used equipartition estimate of magnetic field strengths is more reliable at low frequencies. Here equipartition between the energy densities of magnetic fields and total cosmic rays is assumed. As the cosmic ray energy is generally dominated by protons, another assumption is needed which is the ratio  $K$  between the number densities of protons and electrons in the relevant energy range. This ratio, however, depends on the energy loss processes of the cosmic rays which are much different for protons and electrons (Beck & Krause 2005). At low frequencies energy losses are generally weaker, so that the equipartition estimate has a smaller error.

## 2.2 Polarization and Faraday rotation at low frequencies

The degree of linear polarization of synchrotron emission is a measure of the degree of ordering of the magnetic field. In a fully ordered field, about 75% polarization is expected. Recent observations at radio frequencies of several GHz revealed large-scale ordered magnetic fields in many spiral galaxies and degrees of polarization of up to 50% (Beck 2005, 2007). At low frequencies strong *Faraday depolarization* effects occur along the line of sight and within the telescope beam, caused by ionized gas and magnetic fields in the synchrotron-emitting volume. As the result, the observation of diffuse polarized emission at low frequencies is especially suited to targets with low field strengths and low plasma densities (see Sect. 2.3).

Far away from their sources in galaxies, cosmic-ray electrons have lost most of their energy and no significant synchrotron radiation is emitted. If magnetic fields still exist in those regions and have a significant coherent regular component, they can still be indirectly detected by the effect of Faraday rotation of polarized synchrotron emission from background sources. The *Faraday rotation measure* RM is proportional to  $B_{\text{reg}} n_e \lambda^2$  where  $B_{\text{reg}}$  is the regular <sup>1</sup> field strength along the line of sight and  $n_e$  is the thermal electron density. Hence, RM depends on  $B$  with a smaller exponent than synchrotron intensity  $I$  which further helps to detect weak fields. If the energy densities of magnetic field, cosmic rays and thermal gas all have an exponential decline with distance, e.g. from a star-forming region, with the same scale length  $l$ , the synchrotron intensity  $I$  has a scale length of  $2l/(3 + \alpha)$ , while the scale length of RM is longer and equal to  $2l/3$ .

LOFAR can measure rotation measures (RM) with a very high precision and hence detect weak magnetic fields and low electron densities which are unobservable at higher frequencies. The high RM precision of LOFAR will also help to study RMs from pulsars, stellar and AGN jets, and the gaseous halos of radio galaxies with unprecedented accuracy. With its wide-band polarization capability, LOFAR can measure differences in RM of  $\pm 0.1 \text{ rad m}^{-2}$  of sources detected with a signal-to-noise ratio of 10 in the LOFAR highband (giving  $\pm 36^\circ$  total rotation at 120 MHz and  $\pm 13^\circ$  at 200 MHz). If regions with detectable linear polarization can be discovered also in the LOFAR lowband, even smaller RM differences can be measured. Media with very small RMs are expected to exist in the outermost parts of galaxies and in

---

<sup>1</sup>A *regular* field is defined as a field which has a coherent direction within the volume traced by the telescope beam and hence can give rise to polarized emission and Faraday rotation signals. An *ordered* field can reverse its sign within the telescope beam and hence can be the origin of polarized emission, but without Faraday rotation.

clusters of galaxies.

Estimates of the magnetic field strength mostly rely on the equipartition assumption which may not be valid at small spatial or time scales. Faraday rotation data, in combination with measurements of the *thermal absorption* of the total radio emission at low radio frequencies, will allow us to measure the regular magnetic field strength and the ionized gas density in the plasma clouds along the line of sight.

A grid of RM measurements of polarized background sources is much less affected by Faraday depolarization within the foreground object and hence is a powerful tool to study magnetic field patterns in the disks and halos of galaxies (Stepanov et al. 2008). A sufficiently large number of sources is required to account for the intrinsic RM of extragalactic sources, and to separate the Galactic foreground contribution to RM. In principle, much larger Faraday rotation angles are expected at lower frequencies. Thus, much more tenuous ionized gas and/or much weaker magnetic fields can be measured at low frequencies. The available number density of linearly polarized sources at low frequencies will become known from the LOFAR surveys. Generally, it is expected that at low frequencies the magnitude of achievable fractional polarization is lower. Furthermore, the number density of polarized sources is reduced due to Faraday depolarization effects within the sources and in the foreground.

The assembly of a statistically significant sample of integrated RM measurements along different lines of sight through galaxies and galaxy clusters will permit the study of magneto-hydrodynamical turbulence in these objects to a level of detail that cannot be reached in terrestrial laboratories and supercomputers, nor via analytical calculations. LOFAR will thus open up the study of MHD turbulence in a large number of galactic environments, permitting us to address many of the open questions of MHD turbulence and dynamo theories. The scientific potential of analyzing data from diffuse extended media with *RM Synthesis* (Sect. 2.3) will be even larger.

In summary, LOFAR is *THE* telescope to measure weak cosmic magnetic fields.

## 2.3 Rotation Measure Synthesis

With LOFAR’s high spectral resolution (better than 1 kHz) *Rotation Measure (RM) Synthesis* based on multi-channel spectro-polarimetric data can address almost the whole range of RM values as well as separate RM components from distinct foreground and background regions (Brentjens & de Bruyn 2005). This can be used to analyze the 3-D structure of the magnetized interstellar medium in galaxies (Sect. 4). Some further technical and calibration issues are discussed in Sections 10.1 and 10.2.

*RM Synthesis* Fourier-transforms the complex polarization data from a limited part of the  $\lambda^2$ -space (where  $\lambda$  is the observation wavelength) into a data cube with *Faraday Depth* (FD)<sup>2</sup> as the third coordinate, similar to synthesis of radio images. The distribution of polarized emission as a function of FD may be called “Faraday spectrum”.

The total band and channel width of the observation defines the *Rotation Measure Spread Function* (RMSF). The RMSF is determined by the total frequency range used in the observation (Heald 2009). Cleaning of the data cube with the known RMSF (“dirty beam”) is similar to cleaning of synthesis data (Heald et al. 2009). Figs. 2 and 3 give examples for the RMSF expected for three frequency spans of LOFAR.

---

<sup>2</sup>*Faraday Depth* (FD) is defined as the integral over the line of sight of the thermal electron density multiplied by the component of the regular field strength along the line of sight. FD is a physical quantity and is generally different from the observable quantity *Rotation Measure* (RM), which is the slope of the variation of polarization angle with  $\lambda^2$ . In the simple case of a layer homogeneously filled with magnetic fields, cosmic-ray electrons and thermal electrons, and negligible Faraday depolarization,  $RM = FD/2$ . For a non-emitting magneto-ionic medium in front of a polarized background source (“Faraday screen”),  $RM = FD$ .

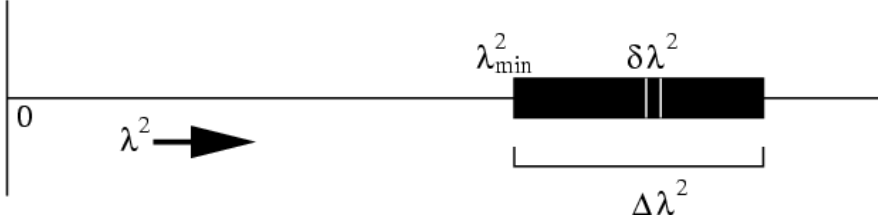


Figure 1: Three instrumental parameters determine the output of a Faraday rotation observation in  $\lambda^2$  space: the minimum wavelength  $\lambda_{min}^2$ , the resolution  $\delta\lambda^2$ , and the total range  $\Delta\lambda^2$  (from Brentjens & de Bruyn 2005).

Three main factors determine the scope of a RM measurement (Fig. 1):

(i) The RM resolution, which is mainly determined by the FWHM of the main lobe of the RMSF (which is approximately of Gaussian shape), given by

$$\delta\phi \approx \frac{2\sqrt{3}}{\Delta\lambda^2}, \quad (5)$$

where  $\Delta\lambda^2$  is the width of the  $\lambda^2$  coverage of the observation. A large range  $\Delta\lambda^2$  increases the RM resolution (Figs. 2 and 3) and also removes the  $n\pi$  ambiguities.

The location of the peak of a Gaussian distribution can be determined to better than the FWHM if the signal-to-noise ratio  $Q$  is high; the position error decreases with  $2S^{-1}$ . Similarly, the RM error decreases linearly with the signal-to-noise  $Q_p$  of the polarization signal integrated over all frequency channels, so that we get

$$\delta\phi \approx \frac{\sqrt{3}}{\Delta\lambda^2 Q_p}. \quad (6)$$

RM Synthesis with LOFAR takes advantage of the wide  $\lambda^2$  range achievable at low frequencies. For example, covering the highband (120–240 MHz) yields  $\delta\phi \approx 0.37/Q_p$  rad  $m^{-2}$ . Hence, LOFAR observations with large signal-to-noise  $Q_p$  will allow the measurement of RM differences well below 1 rad  $m^{-2}$ . In the lowband, the RM accuracy is formally even better – however, calibration is much more difficult and the sensitivity of the antennas is lower.

More generally, the precision with which we can measure the RM of a polarized source depends on the signal-to-noise ratio of the detection as well as on the spread  $\sigma_{\lambda^2}^2$  of the measurements made in the experiment. As described by Brentjens & de Bruyn, we can write the expression for the variance in the observed RM as

$$\sigma_\phi^2 = \frac{\sigma^2}{4(N-2)P^2\sigma_{\lambda^2}^2}, \quad (7)$$

where  $\sigma$  is the noise in a single channel (in Stokes Q or U, assumed to have equal signal-to-noise levels);  $N$  is the number of channels;  $P$  is the polarized intensity of the source; and  $\sigma_{\lambda^2}^2$  is the variance of the distribution of  $\lambda^2$  samples (channels).

(ii) The maximum observable Faraday depth of a non-emitting Faraday screen before bandwidth depolarization within an individual frequency channel becomes important is

$$\phi_{max} \approx \frac{\sqrt{3}}{\delta\lambda^2}, \quad (8)$$

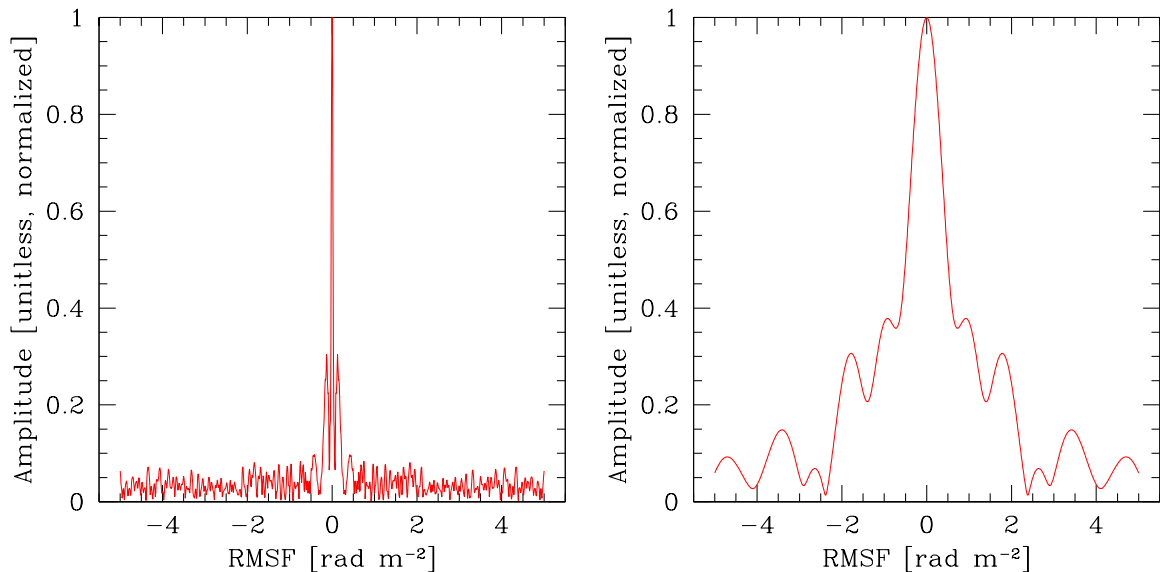


Figure 2: Rotation measure spread function (RMSF) for LOFAR survey observations (according to the plans of the Surveys Key Science Project) in the lowband at 30–50 MHz plus 60–80 MHz (left) and in the highband at 120–150 MHz plus 180–210 MHz (right), both with a total bandwidth of 16 MHz. The RM resolutions  $\delta\phi$  are 0.05 and 1.0  $\text{rad m}^{-2}$ , the maximum observable Faraday depths  $\phi_{max}$  are 19 and 1200  $\text{rad m}^{-2}$ , and the maximum widths in Faraday depth  $L_{\phi,max}$  are 0.2 and 1.5  $\text{rad m}^{-2}$ , respectively (from Heald 2009).

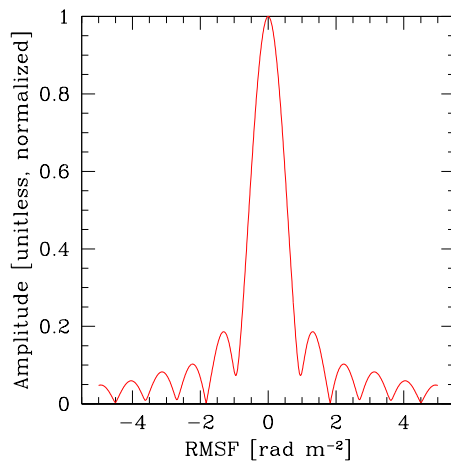


Figure 3: Rotation measure spread function (RMSF) for deep LOFAR observations (according to the plans of the Magnetism Key Science Project) in the highband at 120–180 MHz, with a total bandwidth of 40 MHz. The RM resolution  $\delta\phi$  is 1.1  $\text{rad m}^{-2}$ , the maximum observable Faraday depth is 1200  $\text{rad m}^{-2}$ , and the maximum width in Faraday depth  $L_{\phi,max}$  is 1.1  $\text{rad m}^{-2}$  (from Heald 2009).

where  $\delta\lambda^2$  is the spacing between adjacent  $\lambda^2$  samples (channels). At 120 MHz  $\phi_{\max} \approx 1.7 \cdot 10^4 / \delta\nu$  rad m<sup>-2</sup> where  $\delta\nu$  is the width of an individual frequency channel measured in kHz. The frequency resolution of LOFAR of 0.7 kHz is sufficient to detect even the largest expected Faraday depths in the highband. For constant  $\delta\nu$ , the maximum FD varies rapidly with the observation frequency  $\nu_0$ ,  $\phi_{\max} \propto \nu_0^3$ , so that large FD values are harder to measure in the lowband.

(iii) The maximum observable FD width of a feature which is extended in FD space (i.e. mixed emission and rotation), before strong depolarization occurs, is

$$L_{\phi,\max} \approx \frac{\pi}{\lambda_{\min}^2}, \quad (9)$$

where  $\lambda_{\min}^2$  is the smallest value of  $\lambda^2$  of the observation. This is similar to the “missing-spacings” problem in synthesis imaging. In the LOFAR highband,  $L_{\phi,\max} \approx 2$  rad m<sup>-2</sup>. As a result, polarized emission from dense magneto-ionic regions like the inner galactic disks is hardly observable with LOFAR and needs observations at higher frequencies, e.g. with the SKA and its pathfinders APERTIF, ASKAP and MeerKAT.

The FD data cube contains valuable information about the distribution of regular magnetic fields and ionized gas along the line of sight (*Faraday tomography*). RM Synthesis can only obtain approximate 3-D information due to the non-monotonic relation between physical distance along the line of sight and Faraday depth. Under simple conditions, such as a uniform layer of magnetized ionized gas or a series of individual clouds along the line of sight, Faraday depth and geometric depth are proportional. In such cases, the resulting FD data cube contains more polarized intensity than from a simple addition of all spectral channels because emission from each cloud has been corrected for Faraday rotation. For objects with more complicated structures, e.g. including field reversals or turbulent fields, a 3-D “tomographic” reconstruction will be possible only in some cases, where the additional information on the direction and magnitude of the magnetic field components can be obtained by other means, e.g. using symmetry arguments or modeling.

### 3 Milky Way

Low-frequency Galactic polarization research has two main aspects: one is the study and understanding of the (local) magnetized interstellar medium on tiny scales, the other is the of Galactic polarization as a confusing foreground effect when studying distant extended galactic and extragalactic objects. These two aspects are clearly related, but the scientific aim addressed in this Section is to obtain new insights into the properties of magnetic fields and the interstellar medium in our Galaxy.

#### 3.1 Surveys

Polarized synchrotron radiation from the Milky Way is visible over the whole sky, up to high latitudes, at all radio frequencies. At lower frequencies where Faraday rotation plays an important role, the observed polarization structures are largely different in morphology compared to the corresponding total intensity image due to depolarization in the interstellar medium by Faraday effects. This effect is obvious in Fig. 4, which shows the first all-sky polarization map which was obtained at a frequency of 1.4 GHz at 36′ angular resolution. Extended polarized emission from the intense emission in the inner Galaxy is not visible.

PI at 1.4 GHz (26m DRAO+30m Villa Elisa)

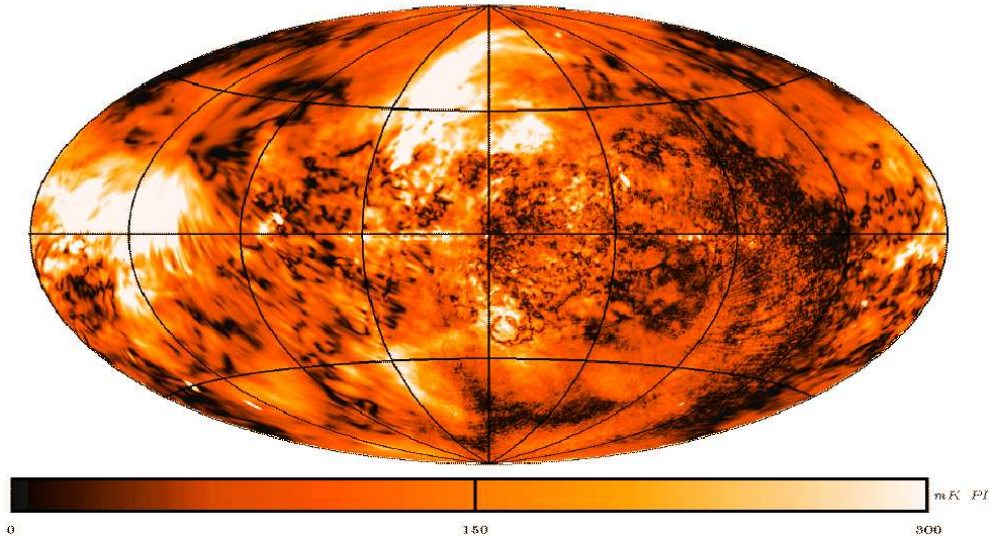


Figure 4: All-sky polarization map at 1.4 GHz at  $36'$  resolution (W. Reich, priv. comm.), combined from northern and southern sky observations with the DRAO 26 m telescope (Wolleben et al. 2006) and the Villa Elisa 30 m telescope (Testori et al. 2008), respectively.

The morphology of the polarization all-sky map changes above about  $30^\circ$  absolute latitudes from patchy to homogeneous structures as they are expected for diffuse Galactic polarization. Towards the inner Galaxy direction, the intensity level of the patchy polarized emission is almost constant, indicating its local origin without contributions from the inner Galaxy.

At high Galactic latitudes, polarization angle and RM variations are low and observations at long wavelengths are needed to trace them. Wide-field low-frequency polarization observations of the Galactic foreground emission at mid-latitudes in the frequency range 300 MHz to 400 MHz have been made over the last 15 years using the WSRT. They show a wealth of unresolved small-scale polarization at angular resolutions down to a few arcmin at intermediate latitudes (Haverkorn et al. 2003, 2004, Schnitzeler et al. 2007).

Bernardi et al. (2009) use the WSRT to demonstrate that structure in diffuse polarization can be abundant and complex at 150 MHz in the LOFAR frequency range at an angular resolution of about  $3'$ . However, Pen et al. (2008) find no diffuse foreground polarization at 150 MHz for larger scales ranging between  $11'$  and  $36'$  to their sensitivity limit of 3 K in a small field of one square degree at mid latitude observed with the Giant Metrewave Radio Telescope (GMRT).

It is obvious from these and other observations that both depth depolarization and lateral (i.e. beam averaging) depolarization effects are affecting the intensity and morphology of diffuse polarized emission at low and mid latitudes in a complex way, even at frequencies as high as 1.4 GHz. At frequencies that are an order of magnitude lower, high angular resolution is therefore essential to mitigate beam depolarization to be able to trace Galactic structures with structure on small angular scales.

At low frequencies, small RM fluctuations cause large variations in polarization angle, making LOFAR very sensitive to fluctuations in weak magnetic fields. RMs of the diffuse Galactic emission close to the Galactic plane based on low-frequency data up to 1.4 GHz (Fig. 5) are rather low and contrast to the much higher RMs from background sources shining through the entire Galaxy. Recent background RM data from the Canadian and Southern Galactic Plane Surveys (CGPS, Brown et al. 2003; SGPS, Haverkorn et al. 2006) list values

ranging up to about  $\pm 500 \text{ rad m}^{-2}$ , while at latitudes higher than about  $30^\circ$  RMs from background sources drop to an absolute level between  $20 \text{ rad m}^{-2}$  and  $40 \text{ rad m}^{-2}$ . A mean RM gradient with latitude of about  $2\text{--}4 \text{ rad m}^{-2}$  per angular degree can be expected for high latitudes far from the Galactic plane (de Bruyn et al. 2006), which is easily resolved by LOFAR.

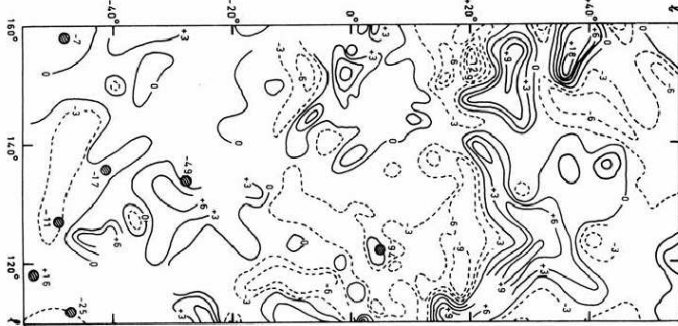


Figure 5: Rotation measure map obtained by Spoelstra (1984) using data from low-frequency polarization surveys made with the Dwingeloo 25-m telescope. It shows a section of  $50^\circ$  in longitude (vertical direction) in the second Galactic quadrant over a range of Galactic latitudes from  $+55^\circ$  to  $-55^\circ$  (horizontal direction). The rotation measure contours of the diffuse Galactic polarization are rather low indicating a local origin, while the RM values (dots) from extragalactic sources are significantly larger (and all negative) as they trace the entire regular magnetic field component along the line of sight across the Galaxy (pointing away from us in this area).

Rotation measure synthesis of the diffuse Galactic synchrotron emission is an excellent way to disentangle various RM components along one line of sight, resulting in a first attempt towards 3-D mapping of the Galactic magnetic field (Sect. 2.3). High Galactic latitudes feature low RM values, ranging from  $\approx 20 \text{ rad/m}^2$  just out the disk down to  $\approx 5 \text{ rad/m}^2$  near the Galactic poles, and only low frequencies permit the appropriate RM resolution. The LOFAR highband will provide a resolution of  $0.1 \text{ rad m}^{-2}$  and the lowband possibly even  $0.05 \text{ rad m}^{-2}$  (see Sect. 10.1). Therefore, LOFAR is uniquely sensitive to small magnetic field and electron density variations in the Galactic interstellar medium, both in the plane of the sky and along the line of sight.

Detailed knowledge of the polarization structure of the Galactic synchrotron foreground is needed for various other science areas. Small-scale RM variations due to diffuse Galactic foreground emission may be of the same order as those observed in the Faraday rotation of extragalactic background (double) radio sources so that characterization of the foreground is necessary to disentangle both contributions. Cosmic Microwave Background (CMB) polarization measurements aim for a sensitivity in polarization fluctuations many orders of magnitude below the fluctuations in Galactic polarization, necessitating detailed knowledge of all polarized foregrounds. In addition, results from modeling of the large-scale Galactic magnetic field (Sect. 3.7) are important to derive the locations of extragalactic sources of ultra-high energy cosmic rays.

Below we will discuss the various research areas within the Milky Way, current data and the way in which LOFAR will contribute.

### 3.2 Faraday screens

*Faraday screens* (Wieringa et al. 1993, Duncan et al. 1999) are structures of strong and

regular magnetic fields, which are usually observable solely through their polarization angle or RM structure. Galactic Faraday screens have been observed using diffuse synchrotron emission at frequencies from 150 MHz to 5 GHz (Gray et al. 1998, Haverkorn et al. 2003, Wolleben & Reich 2004, Sun et al. 2007, Bernardi et al. 2009) and using polarized background sources (Clegg et al. 1992, Whiting et al. 2009). The physical nature or origin of these objects is not entirely clear. Faraday screens are basically “passive” objects, e.g. they do not (or only very weakly) emit in total power or linear polarization. Their signature in polarization is based on their Faraday rotation of diffuse or point source background emission, which adds to foreground polarization in a different way than for the emission offset from the Faraday screen. Candidates for Faraday screens might be very old evolved supernova remnants or old expanded pulsar wind nebulae, where particle injection has stopped but a strong magnetic field is still preserved. The distance of Faraday screens is often not very well constrained. These screens are either very large in size or host excessive regular magnetic fields exceeding the average local Galactic value of about  $6 \mu\text{G}$  by a large factor (see Reich 2006 for a review). Sun et al. (2007) report a Faraday screen with a physical size of 56 pc.

Faraday screens detected at longer wavelengths, where screens with smaller RMs are traced, are most likely of local origin. Low-frequency observations will be sensitive to regular magnetic field structures of smaller sizes and with weaker field strengths and thereby complement the high-frequency observations of Faraday screens containing strong regular magnetic fields.

Understanding and cataloging of Faraday screens is of importance for modeling of the large-scale Galactic magnetic field (see Section 3.7). The existence of such discrete Faraday screens reduces the contribution of the diffuse magneto-ionic medium to the large RMs observed for extragalactic sources in particular in the Galactic plane, and therefore can distort large-scale magnetic field models based on RMs of extragalactic point sources.

### 3.3 The local interstellar cloud (LIC) and the local bubble (LB)

The solar system is embedded in a local bubble of thermal low density gas with a size of about 1 pc and a density of about  $0.1 \text{ cm}^{-3}$  (Frisch 1998, Redfield & Linsky 2007). The LIC properties appear to vary depending on the method applied and the direction of measurements, constrained by local stars.

A density of thermal electrons of  $0.225 \text{ cm}^{-3}$  was reported for the LIC based on low-frequency absorption, where a radial extent of the LIC of about 2 pc was quoted (Peterson & Webber 2002). The LIC is too weak to be traced by  $\text{H}\alpha$  measurements (Reynolds 2004). Polarimetry at the lowest LOFAR frequencies could reveal the thermal density and its fluctuations within the LIC, as well as the magnetic field strength, direction and fluctuations. Determining the properties of the LIC, apart from being interesting in their own right, are also important to allow a proper interpretation of RMs of more distant Galactic structures or intergalactic sources.

The average RM from the LIC is expected to lie in the range of  $0.1\text{--}0.4 \text{ rad m}^{-2}$  for an assumed line of sight magnetic field strength of  $1 \mu\text{G}$ , electron density between  $0.1$  and  $0.2 \text{ cm}^{-3}$  and a pathlength of  $1\text{--}2$  pc. This corresponds to a polarization angle change at 60 MHz of  $5\text{--}19^\circ/\text{MHz}$  or  $3\text{--}12^\circ/10 \text{ MHz}$  at 150 MHz. Fluctuations of the magnetic field and the electron density in the LIC are expected, but the physical scales are entirely unknown. However, from the known global LIC properties RM changes of the order of  $0.1 \text{ rad m}^{-2}$  seem likely. These polarization angle changes are in principle measurable at LOFAR frequencies. Fluctuations of thermal gas density and/or magnetic field on scales of  $0.001\text{--}0.1$  pc cannot be traced by any other methods. Such observations may also bridge the gap to turbulence length scales probed by interstellar scintillation of the intra-day variables sources like J1891+3845,

which point to very local plasma (Macquart & de Bruyn 2007).

On a scale of about 100 pc the distinct local bubble (LB) exists, which is expected to contribute a few RM on average, which LOFAR is able to detect. However, it is difficult to disentangle magneto-ionic LB features from small scale polarization structures with larger distances located in the Milky Way’s halo.

### 3.4 The Galactic halo and disk-halo interface

LOFAR will be an excellent tracer of the magnetized Galactic halo for two reasons: the instrument is sensitive to low RMs and therefore to weak magnetic fields and small field changes, and it can detect old synchrotron electrons very high up in the halo which only emit at low frequencies.

Recent Westerbork RM synthesis observations between 315 MHz and 388 MHz of a high latitude ( $b \approx 70^\circ$ ) field show a rather complex distribution of RM features (de Bruyn et al. 2006). For LOFAR frequencies the complexity is expected to increase. The existence of thermal gas at high latitudes is known from H $\alpha$  surveys and proven by the existence of Faraday rotation, but the source and cause of the gas ionization/excitation is still not well understood. Studies of these high-latitude RM fluctuations could provide more detailed information of the distribution, density and filling factor of the thermal gas, providing clues to its origin.

After identifying “windows” of low Faraday depolarization, LOFAR observations can also help study the structure of the large-scale Galactic field in the halo at mid and high Galactic latitudes. Less affected by ISM turbulence than in the Galactic plane, investigations of these regions can trace the regular magnetic field component and set crucial tests of the dynamo model in action in the Galaxy (see Sect. 4.1). RM Synthesis of the polarized diffuse synchrotron emission will allow us to trace the structure of the Galactic medium along the line of sight resulting in a sort of tomography of the magnetic field.

Low frequency observations carry a further benefit as the emission is provided by low-energy relativistic electrons. Besides representing the bulk of the electron energy budget (so providing more reliable estimates of the energy densities), they are older than those emitting at higher frequencies and can diffuse to larger distances (electrons emitting at 50 MHz can travel 5 times farther than those at 1.4 GHz, see Sect. 2.1). Therefore, we might even be able to probe the Galactic field structure at larger distances accessible at higher frequencies, maybe covering the whole extent of the halo.

### 3.5 Galactic turbulence

Studies of Galactic turbulence demonstrate that turbulent motions are present in both the neutral and ionized medium on a giant range of scales, from AU’s to hundreds of parsecs (e.g. Elmegreen & Scalo 2004, Armstrong et al. 1995). Observational results on the turbulent structure of the Galactic magnetic field are much scarcer. Even though power spectra of fluctuations in neutral and ionized hydrogen gas generally show Kolmogorov-like behavior, power spectra of RM fluctuations also show flatter and/or broken slopes (Minter & Spangler 1996, Haverkorn et al. 2008). Very little is known about sub-parsec structure in the Galactic magnetic field, even though MHD simulations indicate that the bulk of magnetic energy may reside at those small scales (Schekochihin et al. 2004).

LOFAR can make substantial contributions to this research, due to its high spatial resolution and sensitivity to small RM variations. RM Synthesis studies of the diffuse emission allow higher angular resolution than a grid of extragalactic sources.

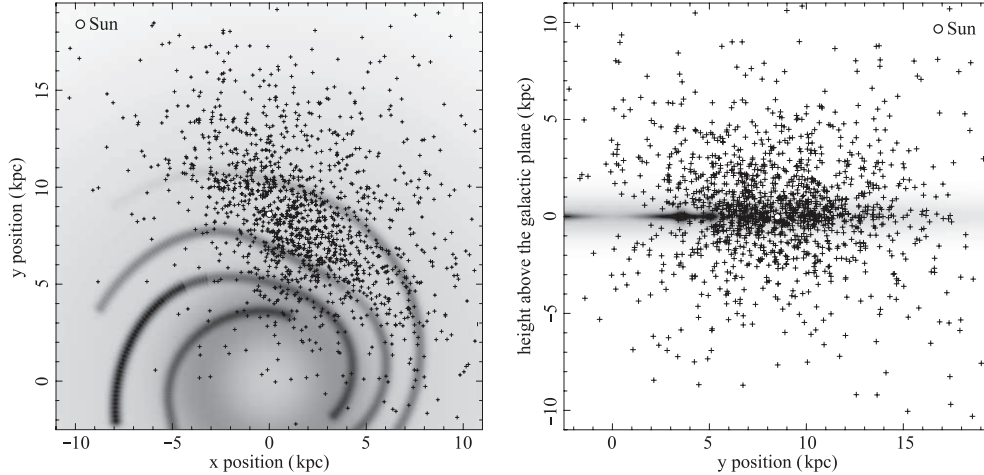


Figure 6: The 1000+ pulsars that LOFAR is expected to find in a 60-day all-sky survey, shown in a Galactic plane projection (left) and an edge-on view of the Galactic plane (right) (from Noutsos et al. 2009).

### 3.6 Pointed Galactic observations

Galactic observations related to Faraday screens, local gas clumps, turbulence and the Galactic halo magnetic field require sufficiently sensitive observations for a number of areas in different Galactic directions. It is difficult to predict a firm number of fields, which will allow place firm statements about the magnetized ISM as a function of Galactic latitude. Therefore, in the first phase Galactic observations will be done simultaneously with observations of nearby galaxies, which fill only a small fraction of LOFAR’s field of view. Nearby galaxy observations will benefit from being corrected for Galactic foreground effects. Based on these results additional areas will be defined to complement the understanding of the Galactic emission. The location of Faraday screens and local gas clumps is unknown and some statistics is expected from the first fields. Other tracers, e.g. very deep  $H\alpha$  images, may become available, which will be used to identify these important components of the magneto-ionic ISM.

### 3.7 The large-scale Galactic magnetic field

The prime way to characterize large-scale structure of the magnetic field such as the pitch angle of the spiral shape or the number and location of large-scale reversals is modeling of the field with input RM values from pulsars, extragalactic (point) sources and being constrained by other data such as the diffuse polarized emission (e.g. Brown et al. 2007, Sun et al. 2008). Defining the structure of the large-scale Galactic magnetic field will aid distinction between different dynamo theories, will enable tracing extragalactic sources of ultra-high energy cosmic rays, constrain galaxy formation theories, and help interpreting the small-scale turbulent magnetic field. LOFAR can make a unique contribution to this dataset by detecting RMs from low-frequency emitting pulsars (Noutsos et al. 2009) and polarized extragalactic point sources with steep spectra, that are too weak to be detected at higher frequencies.

A detailed description of the pulsar program is given by Noutsos et al. (2009).

## 4 Magnetic fields in spiral galaxies

A key question in theories of magnetic field amplification in galaxies is whether magnetic fields were already strong or even dynamically important in the ISM of young galaxies at high redshifts (Sect. 4.1). This can be answered by searching for nonthermal emission and polarization of distant galaxies selected from deep optical surveys, making use of LOFAR's large collecting area and high resolution.

LOFAR polarization observations will also be able to probe extremely weak cosmic magnetic fields in the nearby Universe which hitherto could not be detected. Such fields probably exist in halos of galaxies (Sect. 4.2), between interacting galaxies (Sect. 5.1), in galaxy groups (Sect. 5.2), in dwarf galaxies (Sect. 6), and probably in the intergalactic medium (Sect. 9), especially in large-scale cosmic filaments.

### 4.1 Galactic dynamos

It is now quite generally accepted that galactic magnetic fields cannot be of purely primordial origin, but that they result instead from the amplification of a seed magnetic field by a hydromagnetic dynamo. However, important questions remain regarding the details of the amplification process, the nature of the seed field, and the final configuration of the large-scale (regular) field.

Dynamo theory is based on the concept that the motions of a conducting fluid embedded in a (even minute) magnetic field generate electric currents, which, under favorable conditions, amplify the original magnetic field. In most astrophysical objects, a conducting fluid is present (e.g., the interstellar plasma in the case of galaxies), and its motions involve a combination of large-scale differential rotation and small-scale cyclonic turbulence, which together lead to magnetic field amplification.

A potential obstacle to dynamo action is the requirement that magnetic helicity has to be conserved (Brandenburg & Subramanian 2005). If the dynamo domain forms a closed system, magnetic helicity conservation implies a severe quenching of dynamo action and an extremely slow (resistively limited) saturation of the large-scale field. This problem can be overcome in the presence of open boundaries, when small-scale magnetic helicity is able to flow out of the system, thereby making it possible for the large-scale field to grow and reach saturation at a much faster rate. There is now increasing evidence that galaxies are open systems. Hot gas and cosmic rays from star-forming regions can drive outflows that continuously expel magnetic energy and small-scale magnetic helicity into the intergalactic medium. Such outflows appear to be indispensable for the continuous build-up of large-scale magnetic helicity by the dynamo.

The nature of the seed magnetic field required to initiate the amplification process has not been clearly identified yet. Several possibilities have been put forth in the literature, but none of them can be regarded as conclusive (see, e.g., Widrow 2002 for a review). A first possibility would be that the Universe was directly born with a magnetic field or that some exotic processes during a phase transition in the very early Universe engendered the first cosmic magnetic fields. Along a more classic line of thought, the first magnetic fields could have been produced by a battery effect, either before the recombination epoch, or at the ionization fronts that propagated through the intergalactic medium during the re-ionization epoch, or else during the collapse phase of rotating protogalaxies. Alternatively, cosmic magnetic fields could have originated in active galactic nuclei or in the first generation of stars and supernova remnants and been expelled into the surrounding intergalactic medium (Kronberg 2006) or into the interstellar medium of the host galaxy.

Evidently, the temporal evolution of large-scale galactic magnetic fields and their present-day characteristics (strength, overall morphology, radial structure, azimuthal and vertical

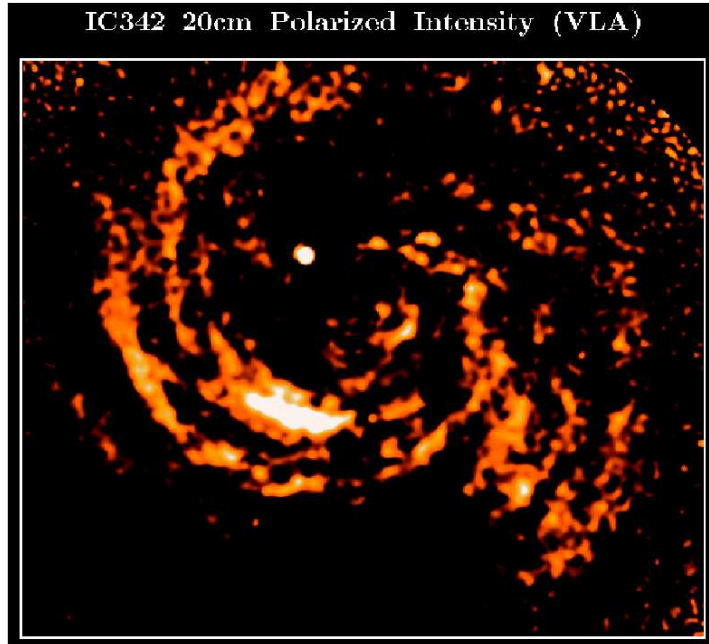


Figure 7: Polarized radio emission of IC 342 at 1.4 GHz, combined from VLA C- and D-array observations, smoothed to  $30''$  resolution. The map size is  $19 \text{ kpc} \times 19 \text{ kpc}$ , assuming a distance of 2 Mpc (from Beck 2005).

symmetry properties, etc) depend on the specifics of galactic rotation and outflows, on the properties of interstellar turbulence and, to a lesser extent, on the type of seed field. The significant uncertainties in all these factors conspire to limit our theoretical knowledge and understanding of galactic magnetic fields. Our present observational knowledge is limited as well by the lack of accurate measurements available for our own Galaxy and by the small number of external galaxies observed with enough spatial resolution to make out their large-scale magnetic pattern.

LOFAR is expected to considerably improve the observational situation in several ways, mainly by allowing for a 3-D study of the local interstellar medium (Sect. 3.1), by giving access to presently unexplored regions both inside and outside of our Galaxy, and by enlarging the current sample of resolved external galaxies. The expected observational advances will in turn make it possible to place constraints on the true conditions of magnetic field amplification and possibly on the origin of the seed field, thereby enhancing our theoretical understanding of galactic magnetic fields.

“Faraday tomography” with LOFAR (Sect. 2.3) will lead to a detailed three-dimensional view of the Galactic interstellar magnetic field. It will also allow direct measurements of magneto-ionic turbulent fluctuations and their spectrum, which will give us a better handle on the properties of the turbulent motions responsible for dynamo action. In addition, if LOFAR manages to detect – and, even better, roughly locate – reversals in the direction of the large-scale disk field, it will provide an independent confirmation of their existence inferred from pulsar dispersion measures. This, in turn, will be an indication that either the large-scale disk field possesses non-axisymmetric modes or the Galactic rotation rate falls off with height (Ferrière & Schmitt 2000).

Another asset of LOFAR will be its ability to probe regions with low electron density and/or weak magnetic fields, such as outer galactic disks and galactic halos. Hence the possibility of mapping out the global field distribution in galaxies out to large distances from

their centers (Sect. 4.2). The resulting maps will give us valuable information on the location of interstellar turbulence and, by implication, on its origin (e.g., supernova explosions, Parker instability, magneto-rotational instability).

LOFAR will open the door to performing statistical studies of galactic magnetic fields and using them to test dynamo theory. In particular, one should be able to determine the dominant azimuthal modes in a large number of galaxies and compare the observed trends with theoretical predictions. For reference, standard mean-field dynamo calculations show that axisymmetric ( $m=0$ ) modes are generally the easiest to amplify (e.g., Beck et al. 1996), except in the presence of an external disturbance such as a companion galaxy (which favors  $m=1$  modes) or a strong underlying spiral pattern (which favors  $m=2$  modes). Likewise, LOFAR should make it possible to measure magnetic fields in outer galactic disks and halos with sufficient spatial resolution to determine their vertical symmetry properties (parity) and again to draw comparisons with theory (Beck 2009). Here, mean-field dynamo calculations indicate that quadrupolar (even parity in  $z$ ) modes are generally preferred in galactic disks, while dipolar (odd parity in  $z$ ) modes may be dominant in galactic halos and near galactic centers (e.g. Brandenburg et al. 1992). This is supported by the analysis of polarization and RM data of the Milky Way (Sun et al. 2008), but not by the observations of the edge-on galaxy NGC 253 (Heesen et al. 2009b).

A failure to detect large-scale magnetic fields in the majority of galaxies would indicate that mean-field dynamo action is unimportant (e.g. due to its long timescale, see below), or that the small-scale dynamo (Arshakian et al. 2009) dominates, or else that the field is shaped by shearing and compressing gas flows (Beck 2006).

A crucial question in all dynamo theories concerns the timescale of magnetic field amplification. While the mean-field dynamo requires  $\gtrsim 10^9$  yr of rapid, stable rotation to produce the observed field strengths,  $\lesssim 10^8$  yr would be sufficient for the small-scale dynamo (Arshakian et al. 2009), which would generate small-scale fields only, or for the cosmic-ray driven “fast dynamo” (Hanasz et al. 2004). Dynamically significant magnetic fields may already have accompanied the formation of young galaxies in the early Universe. A powerful test is provided by a search for synchrotron radio emission of high- $z$  galaxies from deep optical surveys.

Note that distant, unresolved galaxies may still be polarized at low frequencies. Magnetic fields in the outer halos are expected to be oriented mostly perpendicular to the disk (Sect. 4.2) and should generate polarized synchrotron emission of unresolved galaxies (Stil et al. 2009). Interactions between galaxies and ram pressure from the intergalactic medium can also generate a preferred field orientation (Sect. 5.1), leading to non-zero polarized emission of unresolved galaxies.

## 4.2 Outer disks and halos of spiral galaxies

Polarization observations of face-on spiral galaxies show huge magnetic features (Fig. 7) which extend well beyond the star-forming disk. In interacting galaxies or galaxies within dense clusters strong polarized emission is often observed far away from the optical disk (Fig. 17). There is increasing evidence that magnetic fields extend deep into the intergalactic space, but synchrotron emission is weak due to the lack of cosmic-ray electrons far away from the star-forming regions in the disk. The scale length of the total synchrotron emission in the disks of spiral galaxies is typically 4 kpc. For equipartition between the energy densities of magnetic fields and cosmic rays, the scale length of the magnetic energy is about 8 kpc, larger than that of any other energy except that of global rotation (Fig. 8). As magnetic energy is proportional to the square of the total field strength, the scale length of the total field strength is typically 16 kpc. The field becomes more regular in the outer parts of galaxies, so that the scale length of the large-scale regular field is even larger. Faraday rotation measures

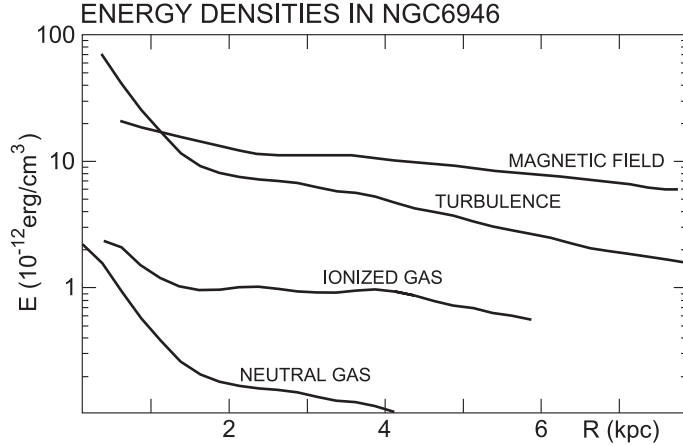


Figure 8: Radial variation of the energy densities of the total magnetic field, turbulent motion of the neutral gas, thermal energy of the ionized gas, and thermal energy of the neutral gas in NGC 6946 — determined from observations of nonthermal and thermal radio continuum, and CO and HI line emission (from Beck 2007).

of polarized background sources behind M 31 showed that the regular magnetic field of this galaxy extends to at least 25 kpc radius (about twice the extent of the optical disk) without significant decrease in strength (Han et al. 1998).

Hot gaseous **halos** of galaxies are a natural result of the collective feedback from massive stars and the subsequent supernovae, and important ingredients for modern scenarios of galaxy formation and evolution. These halos consist not only of thermal warm and hot gas, but also relativistic electrons, which allow the study of the magnetic field topology outside the galaxy disks using radio polarimetry. The magnetic field in return is a critical component influencing the flow of the warm and hot plasma and therefore the matter flow and feedback in galaxies.

Edge-on galaxies possess radio halos of about 2 kpc scale height (Krause 2003). The mean scale height of the total magnetic field is  $\simeq 8$  kpc in case of equipartition between the energy densities of magnetic field and cosmic rays. However, low-frequency maps of edge-on galaxies always show a steepening of the spectral index with increasing height (e.g. Hummel & Dettmar 1990) which indicates energy losses of the cosmic-ray electrons originating in the disk and propagating into the halo. In this case, the scale height of the magnetic field is even larger than according to the equipartition assumption.

The orientations of the field near the midplane are mainly parallel to the disk, but with increasing vertical components with increasing distance from the midplane (Fig. 10). If star formation in the disk is very strong, the vertical field can be dominant already near the plane, as in the central part of NGC 4631 (Krause 2009, Fig. 12).

NGC 253 hosts the brightest and nearest edge-on galaxy in the sky (but unfortunately cannot be observed with LOFAR due to its southern declination). It was recently studied in unprecedented detail with help of high-sensitivity Effelsberg and VLA observations at 4.8 and 8.4 GHz (Heesen et al. 2009a, 2009b; Fig. 11). The local scale height of the radio halo (at different distances from the galaxy’s center) decreases with increasing magnetic field strength, i.e. the halo extent is limited by synchrotron losses of the cosmic-ray electrons (CREs). The scale height of the radio halo of NGC 253 increases towards lower frequencies (1.4 GHz and 300 MHz). This result confirms the prediction that the losses decrease and the lifetime of the electrons increases with decreasing frequency (see Sect. 2.1). Measurements of the halo scale heights at different locations and wavelengths and estimates of the CRE lifetime from

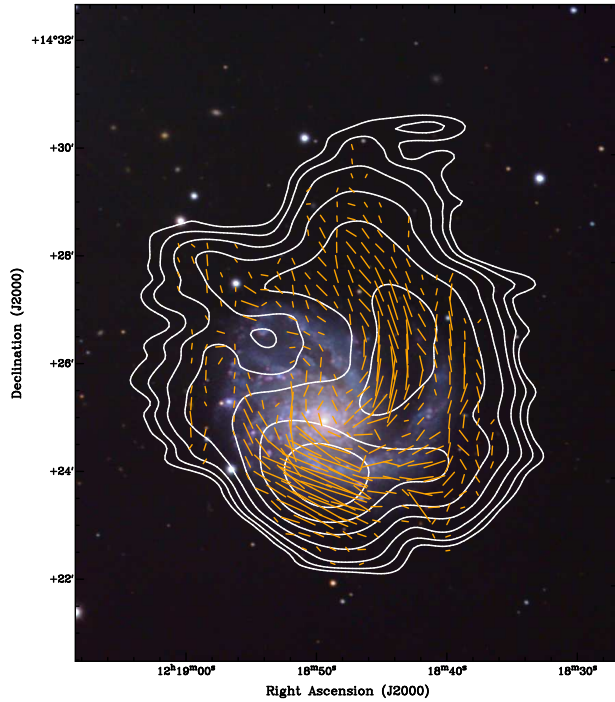


Figure 9: Contours of polarized flux (at  $60''$  resolution) and  $B$ -vectors (corrected for Faraday rotation) overlaid on the optical image of NGC 4254 (image courtesy of Robert Gendler). The 1.37 GHz and 1.70 GHz radio data shown here are from the WSRT-SINGS survey (Heald et al. 2009). Vector lengths are proportional to the polarized flux. The spiral pattern extends far to the north of the optical disk.

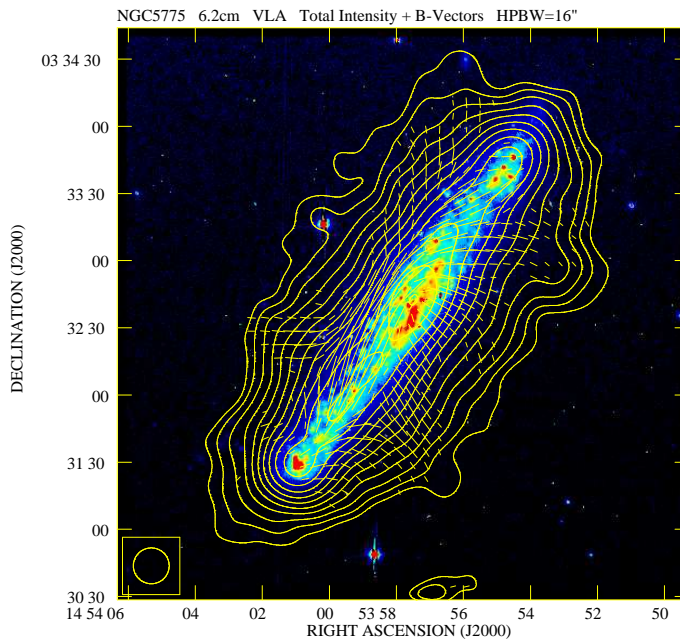


Figure 10: Total radio emission (contours) and apparent  $B$ -vectors of NGC 5775 at 4.8 GHz ( $16''$  resolution), observed with the VLA. Vector lengths are proportional to the polarized intensity (from Tüllmann et al. 2000). Note that the vector orientations in this and all following figures are not corrected for Faraday rotation, which is small at frequencies of 4.8 GHz and higher.

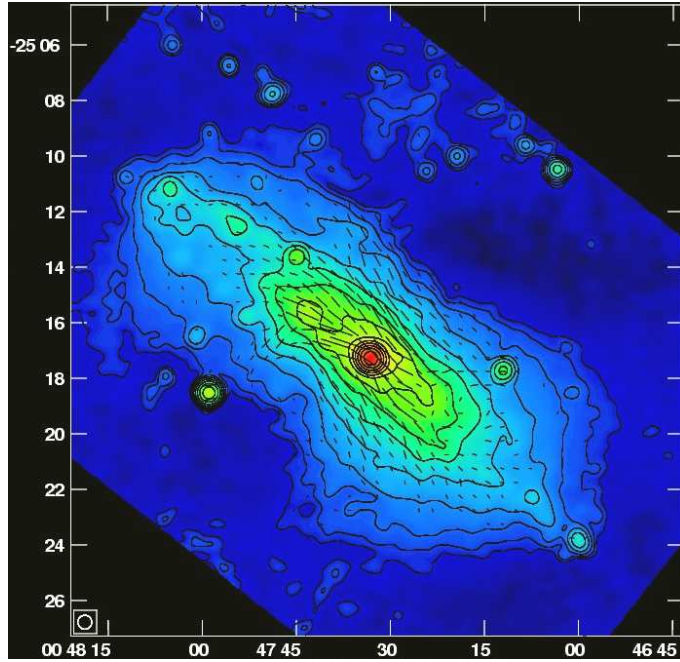


Figure 11: Total radio emission at 6 cm wavelength (30'' resolution) and  $B$ -vectors of the almost edge-on spiral galaxy NGC 253, combined from observations with the VLA and the Effelsberg 100m telescope (from Heesen et al. 2009a,b).

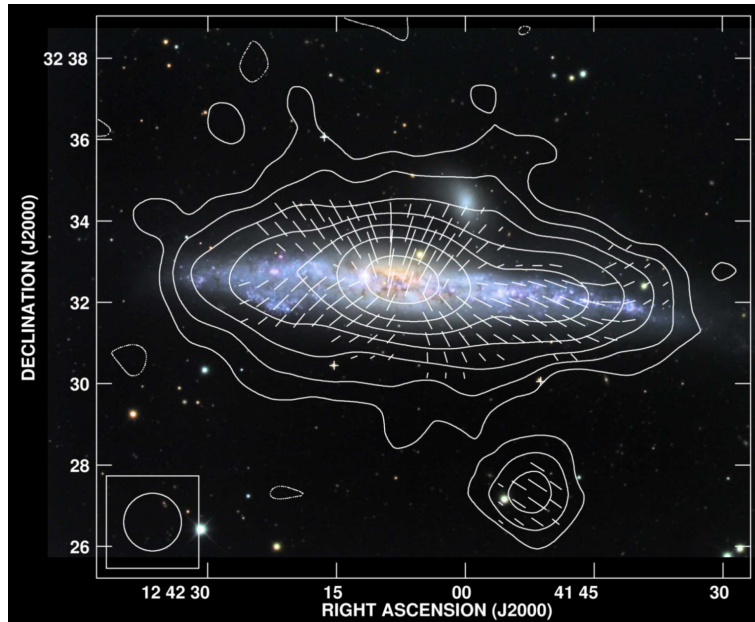


Figure 12: Total radio emission (contours) and  $B$ -vectors of NGC 4631 at 8.35 GHz (70'' resolution), observed with the Effelsberg 100m telescope. Vector lengths are proportional to the polarized intensity (from Krause 2009).

field strengths allowed us for the first time to measure the *average vertical bulk speed* of the CREs ( $300 \pm 30$  km/s) in the northern part of the galaxy (Heesen et al. 2009a). This is significantly larger than the Alfvén speed in the halo (about 150 km/s), so that an outflow of gas transporting the cosmic rays and the magnetic fields is required. In the southern part of NGC 253, the data indicate that diffusion of CREs into the halo dominates over convection.

Magnetic fields in galaxy halos can also be detected via Faraday rotation. Dynamo models predict dipolar or quadrupolar magnetic fields in galactic halos (Sect. 4.1), which should generate large-scale patterns in the distribution of RMs. With regular field strengths  $B \simeq 1\text{--}10$   $\mu\text{G}$ , thermal electron densities  $n_e \simeq 10^{-3}$   $\text{cm}^{-3}$  and pathlengths  $L \simeq 1$  kpc, RM values of  $1\text{--}10$   $\text{rad m}^{-2}$  are expected. Observations of RMs of the diffuse polarized emission from the halos of a few nearby edge-on galaxies at GHz frequencies revealed values in this range, but with large error bars due to the weak emission at high frequencies.

The highest sensitivity of halo observations was achieved for NGC 253 and enabled for the first and only time to measure the RMs from the large-scale fields in the disk and in the halo (Heesen et al. 2009b); both are symmetric with respect to the plane of the galaxy and hence part of a quadrupolar field. The horizontal field in the disk of NGC 253 has an axisymmetric azimuthal component and an inward-directed radial field component.

NGC 4631 hosts an exceptionally bright halo, so that rotation measures could be measured with relatively high accuracy. Still, the RMs do not reveal any systematic pattern. The magnetic field in the halo is neither quadrupolar nor dipolar, as predicted by dynamo models, but is “X-shaped” (Fig. 12). This structure may be related to outflows of gas and magnetic fields.

Present-day radio data are not sensitive enough. The measurement of RM patterns with LOFAR will offer a direct test of dynamo action in galaxies (Beck 2009). LOFAR will allow measurements of many more galaxies with much higher precision than those presented above, also using polarized background sources (see below). Measuring the Faraday rotation and knowing the ionized gas density from X-ray and H $\alpha$  data, we will also determine the regular magnetic field strength independently of the equipartition assumption.

Another powerful tool to search for magnetic fields away from cosmic ray sources (e.g. high in galactic halos) is to measure a grid of Faraday rotation measures towards polarized background sources. Existing instruments do not provide enough sensitivity to detect a sufficiently large number of polarized sources shining through the halos even in nearby galaxies. To recognize large-scale field structures, at least 10 background sources within the solid angle covered by a galaxy are required (Stepanov et al. 2008). The estimated surface density of background sources seen by LOFAR will, for the first time, enable systematic studies for a large number of targets.

LOFAR will allow us to trace the topology of magnetic fields in the outer disks and halos of galaxies to much larger distances from the star-forming regions and will provide a much more detailed picture of the interplay of the thermal and non-thermal constituents of galaxy halos. The bulk propagation speed of cosmic-ray electrons and its variation with distance from the star-forming regions can be determined. LOFAR will also allow the detailed study of the magnetic field structure in the halos of galaxies with low star-formation rates. This would help us to understand the relationship between the efficiency of magnetic field generation and the star-forming activity down to low surface brightness and hence the understanding of the causes of low star-formation rates, such as a possible lack of magnetic instabilities.

We plan deep polarization observations of the following galaxies: <sup>3</sup>

---

<sup>3</sup>This list is not a statistically complete sample. It includes galaxies with high radio surface brightness, significant polarization, medium to high star formation rate, which were successfully studied at high frequencies.

- The  $\simeq 5$  best cases from a list of 11 mildly inclined with optical sizes of more than about  $7'$ , declination  $> 0^\circ$ , inclination  $< 60^\circ$ , Galactic latitude  $|b| > 20^\circ$  (the best cases will be chosen based on the results of the survey):  
M 51, M 81, M 101, IC 342, NGC 2403, 2903, 3359, 3953, 4258, 4736, 6946
- The  $\simeq 5$  best cases from a list of 9 strongly inclined (edge-on) galaxies with optical sizes of more than about  $5'$ , declination  $> -1^\circ$ , inclination  $> 75^\circ$ , Galactic latitude  $|b| > 20^\circ$ :  
M 82, NGC 891, 3079, 4217, 4565, 4631, 4666, 5775, 7331
- M 31 and M 33, the largest galaxies on the northern sky.

## 5 Perturbed galaxies and their groups

Compressing and shearing by gas flows can modify the structure of galactic and intergalactic magnetic fields. In particular, regular fields can become aligned along the compression front or perpendicular to the velocity gradients. Such flows also make random fields highly anisotropic (though still with frequent reversals of field direction). As the emission of polarized synchrotron radiation is unchanged by field reversals, the radio emission from anisotropic fields can also be highly polarized, with B-vectors parallel to the compression front. Discrimination between regular and compressed random fields possible is through Faraday rotation measures (RM) — while anisotropic random fields have a zero rotation measure, only the regular ones cause Faraday rotation. In normal galaxies the polarized emission serves as an ideal tracer of compression in spiral arms and bars (e.g. Patrikeev et al. 2006, Beck et al. 2005). Galaxies strongly perturbed by their environment exhibit various anomalies of their gas dynamics, including intense (magnetized?) outflows into the intergalactic space. For such objects polarization observations of their magnetic fields provide a sensitive diagnostic tool to detect perturbations of the gas flows *in the sky plane*, not measurable in radial velocity studies (Urbanik 2005).

### 5.1 Tidal interactions of galaxies and IGM ram pressure

The magnetic signatures of compression and shearing effects are best visible in galaxies interacting with their neighbors or with the intracluster gas. In both cases the peculiar gas motions give rise to strong asymmetries in polarized emission. For tidally interacting galaxies, bright polarized ridges or peculiar magnetic arms crossing the optical ones are observed (Fig. 13). The HI data often show impressive tails or intergalactic bridges of ejected neutral gas (Haynes et al. 1979, Clemens et al. 1998; Figs. 13 and 14).

Tidal interactions are also frequent in clusters of galaxies, as they are there more tightly packed in space than the field objects. The heavily disrupted galaxy NGC 4438 (Vollmer et al. 2007) has almost its whole radio emission (total power and polarized, Fig. 15) displaced towards the giant elliptical M 86 to which it is also connected by a chain of H $\alpha$ -emitting filaments embedded in the X-ray gas (Kenney et al. 2008).

The tidal tails from interacting galaxies may also constitute a significant source of intergalactic and intracluster magnetic fields, found to be surprisingly strong (see reviews by Kronberg 2002, 2003). Chyży & Beck (2004) found that in the colliding galaxy pair NGC 4038/39 (Fig. 16) the magnetic field in the gaseous and radio tail becomes more regular, as it is carried

---

A statistically complete sample will be observed in cooperation with the Surveys Key Science Project (see Section 10).

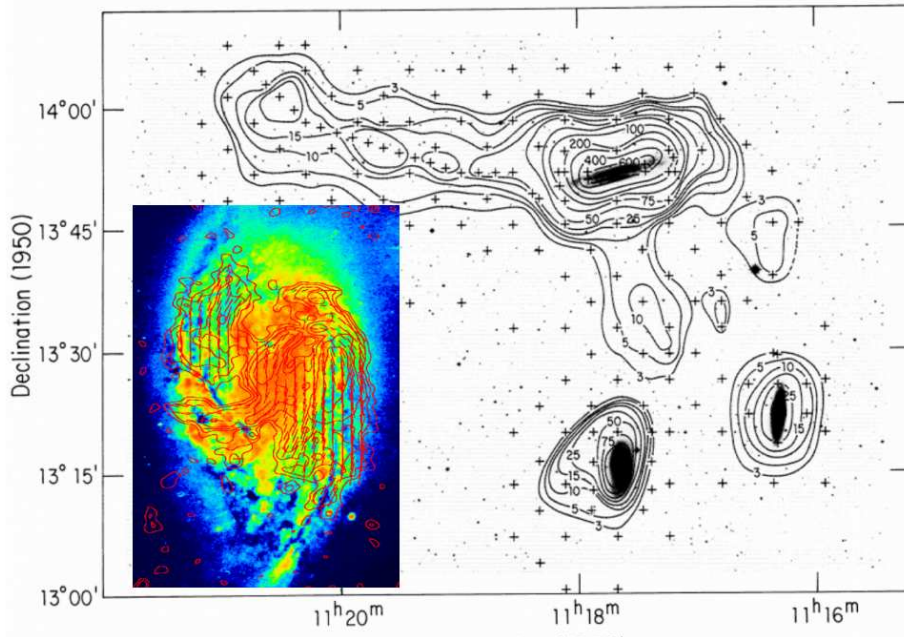


Figure 13: Large image: Contours of extended HI emission around the Leo Triplet, overlaid onto the optical emission (from Haynes et al. 1979). Small image: Contours of polarized emission and  $B$ -vectors of the spiral galaxy NGC 3627, observed at 8.46 GHz with the VLA, overlaid upon the DSS blue image. Vector lengths are proportional to the polarized intensity (from Soida et al. 2001).

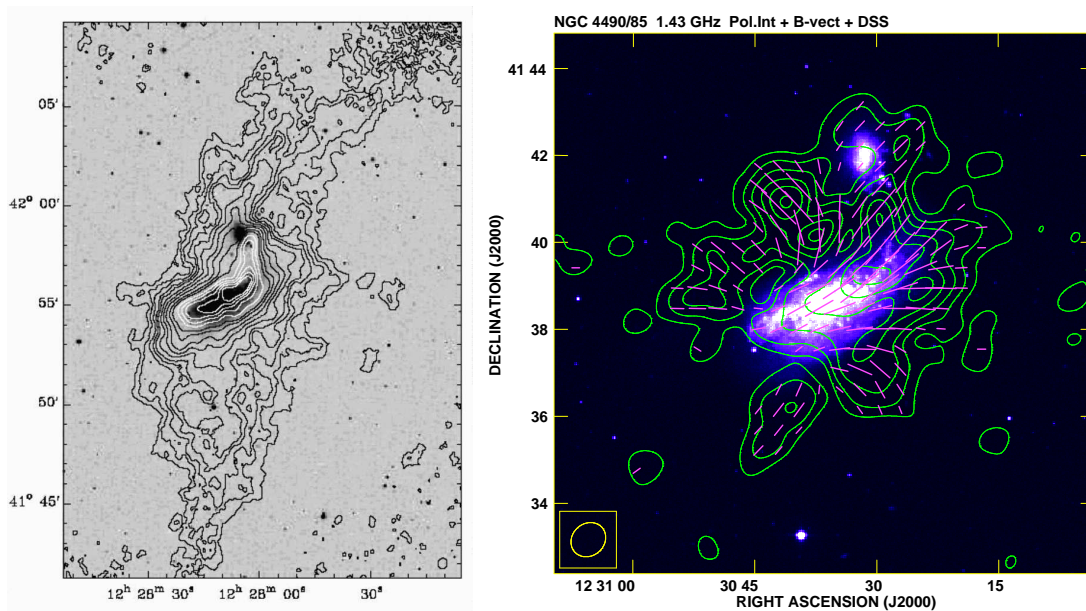


Figure 14: Left: Contours of extended HI emission around the interacting galaxy pair NGC 4490/85, overlaid onto the optical emission (from Clemens et al. 1998). Right: Contours of polarized radio emission at 1.4 GHz with  $B$ -vectors. Vector lengths are proportional to the polarized intensity (VLA data, from Knapik et al. in prep.).

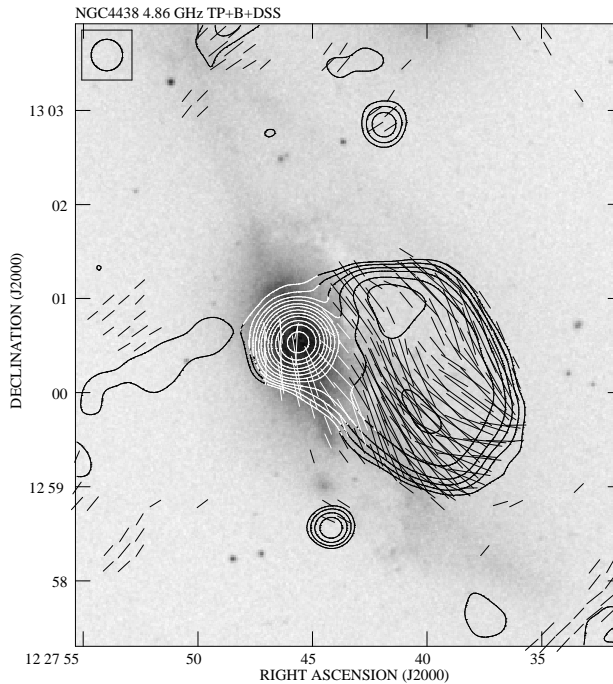


Figure 15: Highly asymmetric 8.46 GHz total power emission as contours and  $B$ -vectors, overlaid upon the blue DSS image of the Virgo Cluster spiral galaxy NGC 4438. Vector lengths are proportional to the polarized intensity (from Vollmer et al. 2007).

away from star-forming regions. The radio spectrum of the tail also steepens dramatically with distance from the cosmic ray sources in the star-forming disk. This makes its outer parts hard to observe at high frequencies.

In a few cases a radio and gaseous bridge has been found between colliding galaxies. In the known cases the radio spectrum steepens there to  $\alpha \simeq 1.4$  ( $S_\nu \propto \nu^{-\alpha}$ ) with a low FIR/radio ratio (Condon et al. 1993, 2002) and little star-formation activity between the galaxies (Zhu et al. 2007). Thus, the bridge radiation is due to relativistic electrons pulled out from the disks together with gas and magnetic fields. The bridge fields are strong enough to affect both the thermodynamics and the bulk dynamics of the bridge gas (Condon et al. 2002). These authors claim this phenomenon (called “taffy galaxies”) to be a rare because only 2 objects, UGC 12914/5 and UGC 813/6, were found so far. This may be due to the steep spectrum of the bridges, making them invisible at centimeter wavelengths for weaker objects. At least one such object has long HI tails (Condon et al. 1993, 2002, see also Gao et al. 2003) of yet unknown radio continuum properties, probably having an extremely steep spectrum. In such cases LOFAR observations can trace cosmic-ray electrons with low energies and weak magnetic fields in the IGM, providing information on the amount and structure of magnetic fields ejected to the intergalactic space during the interactions.

We plan to observe the following tidally interacting galaxies suitable for a deep search of steep-spectrum magnetized tails:

- NGC 3627 — a Leo Triplet galaxy with a strong asymmetry in polarized intensity (Soida et al. 2001). In the western disk the  $B$ -vectors follow the optical spiral pattern, while on the eastern side the magnetic arm crosses the optical one at a large angle (Fig. 13). The galaxy has a steep HI gradient on the western disk edge (where also a bright polarized spot is observed) with a gaseous appendage extending to the east (Haynes et al. 1979).

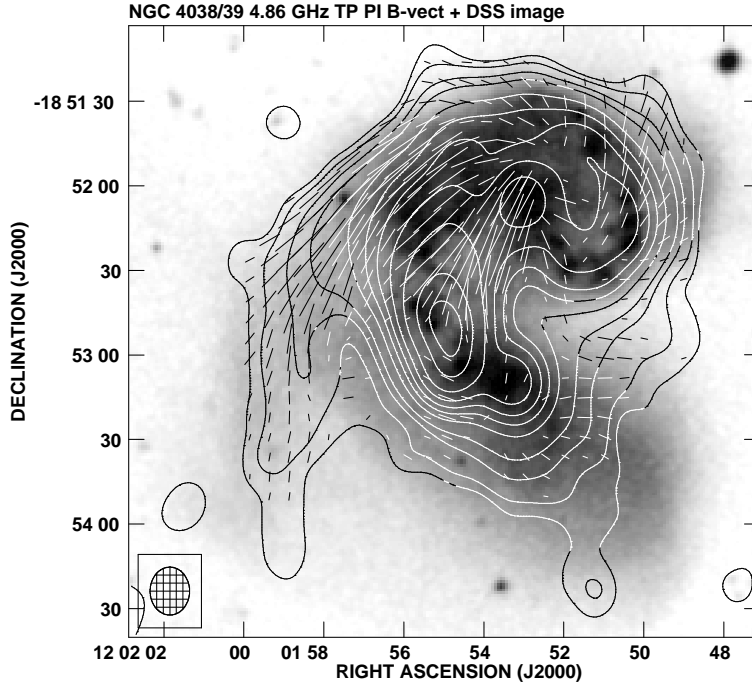


Figure 16: Contours of total radio intensity and apparent  $B$ -vectors of polarized intensity (not corrected for Faraday rotation) of the Antennae galaxies at 8.44 GHz, made from a combination of VLA and Effelsberg data with a resolution of  $17'' \times 14''$ , overlaid upon a DSS image. Vector lengths are proportional to the polarized intensity (from Chyży & Beck 2004).

- NGC 4490/85 — a closely interacting pair of a late-type spiral and a small irregular galaxy. Clemens et al. (1998) found very long HI tails extending perpendicular to the disk of the spiral galaxy (Fig. 14). Knapik et al. (in prep.) found a magnetic bridge between the galaxies and a polarized plume extending from the disk toward the NE with vertical magnetic fields (Fig. 14).
- NGC 4414 — a flocculent galaxy, with a smooth optical appearance and axisymmetric velocity field, thought to be an isolated object. Nevertheless, its polarization picture shows clear signs of interactions with an invisible object, possibly like the dark galaxy VIRGOHI in the Virgo Cluster (Minchin et al. 2007): a bright spot of polarization in the northern disk with almost azimuthal  $B$ -vectors and a large magnetic pitch angle in the southern disk (Soida et al. 2002). The galaxy also shows a small total power tail toward the south, detected at 1.4 GHz, but invisible at higher frequencies. (How steep is the spectrum? How far does it extend?)

In addition to frequent tidal interactions causing distortions of their magnetic fields, cluster galaxies undergo ram-pressure stripping by the intracluster medium (Vollmer et al. 2004a, 2004b, 2008), often in combination with tidal effects. This leads to highly polarized compressional fronts (Vollmer et al. 2008) and gives rise to long gaseous tails on the disk side opposite to the compressed one (Chung et al. 2007). Current radio observations made usually at high frequencies ( $\geq 1.4$  GHz) reveal only few examples of such synchrotron tails (see e.g. Vollmer et al. 2004b). This is due to the rapid steepening of the radio spectrum as the CR electrons age while being carried away from the star-forming disk. To understand the supply of magnetic fields to the intracluster space it is essential to study the magnetic fields carried away from cluster galaxies via various kinds of gaseous tails. A sensitive radio and polarization

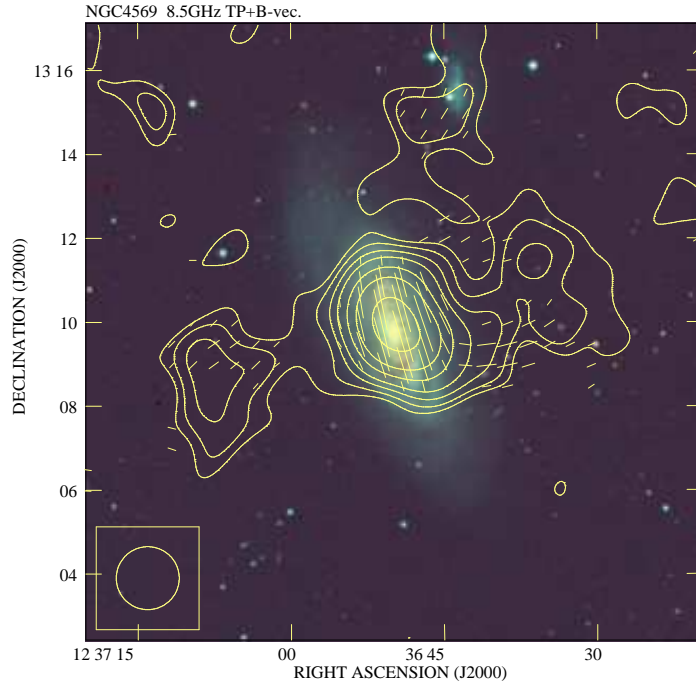


Figure 17: Contours of total emission and  $B$ -vectors of the spiral galaxy NGC 4569, observed at 8.45 GHz and  $90''$  resolution with the Effelsberg telescope. Vector lengths are proportional to the polarized intensity (from Chyży et al. 2006).

study of cluster galaxies at very low frequencies using LOFAR would greatly help to solve this problem.

Another issue is the large-scale outflow of magnetized hot gas from strongly stripped, anemic cluster galaxies, showing presently low star-formation rates and very weakly active nuclei. The cause is not known (stripping, past starburst, past nuclear outburst?). Only one such case, NGC 4569, has been studied in detail so far (Fig. 17). These radio outflows are also subject to ram pressure effects, have generally steep radio spectra ( $\alpha > 1$ ) and are difficult to detect in high-frequency observations. A sensitive search of such phenomena at low frequencies is highly desirable.

We plan to observe the following Virgo Cluster spirals undergoing various combinations of ram pressure and tidal effects:

- NGC 4654 — This galaxy shows a long HI tail toward the SE (Phookun & Mundy 1995). The polarized flux peaks at the base of the tail and extends along it (Vollmer et al. 2007).
- NGC 4438 — A heavily perturbed galaxy: its extended total power and polarized emission are displaced westwards from the optical disk (Vollmer et al. 2007). The galaxy is connected to M 86 with an X-ray bridge containing embedded H $\alpha$  filaments (Kenney et al. 2008).
- NGC 4396 — This almost edge-on galaxy shows an HI tail to the NE (Chung et al. 2007) coincident with the radio continuum extension (Vollmer et al. 2007 plus an unpublished total power VLA map).

- NGC 4522 — A heavily stripped galaxy (Vollmer et al. 2004b) with the disk compressed along its SE side and a one-sided radio halo extending to the NW.
- NGC 4535 — This apparently normal, barred galaxy in the southern extension of the Virgo Cluster shows a dramatic asymmetry in polarized emission (Weżgowiec et al. 2007). Almost all polarized flux comes from the western spiral arm. Finding any steep-spectrum tails or envelopes would solve the question of cause of the polarization asymmetry.
- NGC 4569 — An anemic, HI-deficient galaxy showing little star formation and a very weak LINER source in the center. Nevertheless, it possesses large, steep-spectrum lobes (Chyży et al. 2006) of yet unknown origin. They are accompanied by a huge X-ray halo (Weżgowiec et al. in prep.).

## 5.2 Galaxy groups

In compact galaxy groups tidal interactions may trigger rapid star formation in one or more member galaxies, causing supersonic outflows of the hot gas (Strickland et al. 2004). In tight galaxy groups these gas flows collide and give rise to shocks in the gas already present in the intra-group space. Indeed, some of galaxy groups contain intergalactic gas pools with 40–50 kpc long collisional shock fronts. It is already known that some compact groups have long HI tails, indicating strong, tidally driven outflows of the neutral gas from the system (Williams et al. 2002). Long HI plumes and bridges are also frequently observed in more loose galaxy groups (e.g. Leo Triplet, Haynes et al. 1979). If the expelled gas was magnetized it might provide the supply of magnetic fields into the intergalactic space. Given the lack of strongly active galaxies in groups, the starburst galaxies (either dwarf and massive) constitute the basic source responsible for the “enrichment” of the intra-group medium with relativistic particles and magnetic fields. There are grounds to expect that the compact galaxy groups show diffuse radio emission, with a spectrum rapidly steepening away from cosmic-ray sources in galactic disks.

Bertone et al. (2006) used cosmological simulations to demonstrate that starburst galaxies are able to magnetize the high-density regions of the cosmic web up to field strengths of  $10^{-12} < B < 10^{-7}$  G. Such works only consider the effects of ensembles of individual winds from starburst dwarfs and more massive galaxies, while the additional effects of interaction of winds are neglected. In galaxy groups, especially in compact ones, this is a severe oversimplification. First, the acceleration time in long shock fronts (tens of kpc) allows speeding up the cosmic rays to energies much higher than the galactic cosmic ray (CR) sources in individual galaxies (Siemieniec-Ozieblo & Ostrowski 2000). Moreover, shocks and shearing flows caused by outflows and colliding galactic winds may lead to amplification and ordering of magnetic field in the intra-group medium, as well.

Taking all the above, studying compact groups of galaxies with LOFAR will bring essential information on the following issues:

1. How much of the magnetic flux is carried away from the groups (either compact or more loose) with the various phases of the escaping gas, contributing to the general intergalactic field? This needs a sensitive search for steep-spectrum halos or tails caused by carried-away magnetic fields illuminated by aging electrons. We want to know how the magnetic fields are modified by shocks and shearing flows (as diagnosed by polarization observations) before escaping to the extragalactic space. Extending the radio spectrum of shocked regions down to the lowest electron energies will provide a detailed insight into the CR acceleration in such structures.

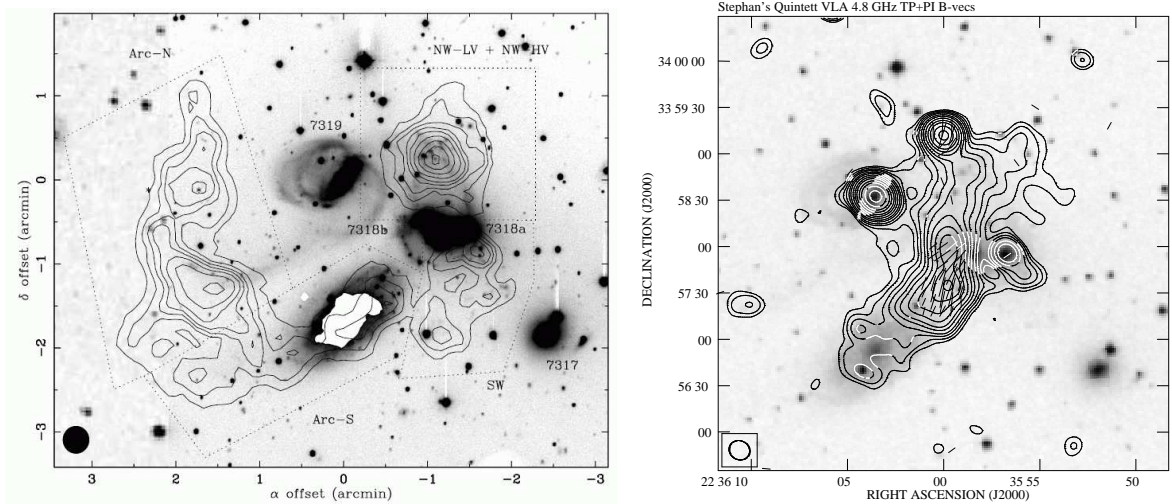


Figure 18: Left: HI tail around Stephan’s Quintet (from Williams et al. 2002). Right: Contours of the total power and  $B$ -vectors of Stephan’s Quintet observed with the VLA at 4.86 GHz, overlaid upon the blue DSS image. Vector lengths are proportional to the polarized intensity (from Soida et al. in prep.).

2. Inclusion of the magnetic and CR pressure may change the estimates of dark matter content of galaxy groups using the hydrostatic equilibrium (e.g. Gastaldello et al. 2007). This is in turn crucial for estimates of the mass parameter  $\Omega_M$ . A full physical picture of all these phenomena still lacks important information: What are the strength and structure (thus pressure and energy density) of intra-group magnetic fields? These are the clues to understand the role of magnetic forces (anisotropic, as it follows from the magnetic field geometry) in the dynamics of intergalactic gas reservoirs. We note that quite a large amount of energy may be stored in diffuse, steep spectrum cocoons invisible to high-frequency observations (like in radio galaxies). Extending the spectrum of CR electrons to low energies is crucial as they may yield a dominant contribution to the overall energy budget. This needs sensitive low-frequency radio and polarization studies.

Compact and loose galaxy groups constitute a unique laboratory of intergalactic plasma and magnetic field production for intergalactic space. We also note that the ionized intra-group ionized gas is so tenuous that rather low Faraday rotation measures are expected which can only be measured at low frequencies.

The best (if not only) well-studied example of a compact group is Stephan’s Quintet (SQ, at a distance of 85 Mpc), with its pool of hot gas extending between the galaxies. It has been claimed by Trinchieri et al. (2005) to be an excellent laboratory of intragroup gas. An intergalactic shock front extending  $\simeq 40$  kpc is traced by the IR-emitting molecular gas (Appleton et al. 2006). This feature can be partly driven by the supersonic motion of the intruder galaxy through the already present intergroup medium, as shown by Trinchieri et al. (2005), and makes SQ an object of particularly interesting physics.

Stephan’s Quintet shows a huge, long filament visible in radio continuum (Xu et al. 2003). Strong polarization of this intragroup emission (Soida et al. in prep, Fig. 18) indicates a substantial content of ordered (regular or shock-compressed random) magnetic fields.

We propose the following objects for a low-frequency search of steep-spectrum intergalactic emission and magnetized tails or cocoons:

- Stephan’s Quintet — a compact galaxy group (also called HCG 92) at a distance of 85 Mpc, perturbed by a high-velocity intruder. It has a pool of a hot gas extending between the galaxies. High-frequency observations also show intergalactic emission (Xu et al. 2003) which is partly polarized (Soida et al. in prep., Fig. 18).
- Other promising targets showing clearly visible intergalactic radio continuum emission in NVSS are the compact groups HCG 15, 44, 57, 62, and 97.
- The Leo Triplet (in addition to NGC 3627 described above) — a loose galaxy group with long HI bridges and plumes extending over the intragroup space (Haynes et al. 1979, Fig. 13). We plan a deep search for low-frequency radio emission and polarization from these gaseous tails and from possible low-frequency cocoons and magnetized outflows, which are rarely seen at high frequencies (e.g. in NGC 4569, Fig. 17).

## 6 Dwarf galaxies

Kronberg et al. (1999) were the first to raise the question of whether low-mass galaxies could have made a significant contribution to the magnetization of the IGM (apart from more massive starburst galaxies and AGNs). According to the standard bottom-up scenario, primeval dwarf galaxies must have been very numerous and injected much of their ISM into the IGM during the initial bursts of star formation. Furthermore, dwarf starburst galaxies are the best local proxies of high-redshift protogalaxies. Total power and polarization observations of these objects will provide input for the interpretation of polarized sources in deep radio survey fields. Such studies are of great importance for cosmology.

Dwarf galaxies are known for their poor containment of magnetic fields and CR electrons (Klein et al. 1991). Apparently, their shallow gravitational potentials fail to confine the relativistic gas during episodes of rapid star formation. Strong galactic winds are present in some prototypical local low-mass galaxies. In fact Martin (1998) found that the outflow velocities in NGC 1569 exceed the escape speed.

Despite their poor confinement of cosmic rays and magnetic fields, the nearby dwarfs are substantially magnetized. The Large Magellanic Cloud was investigated via polarization mapping (Klein et al. 1993, Gaensler et al. 2005a) and via RM studies of polarized background sources (Gaensler et al. 2005b). Skillman & Klein (1988) presented a radio continuum study of the blue compact dwarf galaxies I Zw 36 and II Zw 70 from 325 MHz to 10.7 GHz. A careful analysis of their spectra clearly reveals synchrotron radiation (and hence magnetic fields), especially at low frequencies. Klein et al. (1996) investigated the thermal and nonthermal radio emission in the prototypical starburst dwarf galaxy NGC 4449, finding for the first time a large-scale magnetic field and an extended synchrotron halo. Chyży et al. (2000) analyzed the structure of the magnetic fields in this object, discovering radial “fans” in the central region and fragments of a spiral pattern in the galaxy’s outskirts.

The prototypical low-mass starburst galaxy NGC 1569 was thoroughly studied by Kepley et al. (2009); they found a clear observational evidence of an overall radial magnetic-field morphology, enabling cosmic rays to escape into the halo. Some magnetic fields are likely to be carried away as well. The radio envelopes can best be detected at low frequencies, since the CR electrons age as they travel outwards in the halo, yielding a gradually steepening spectrum. LOFAR is an ideal instrument for this purpose. In a cluster or group environment, such halos are likely to trail behind the galaxy as it moves in the cluster potential with speeds much larger than the diffusion speed of the relativistic particles. This will actually provide

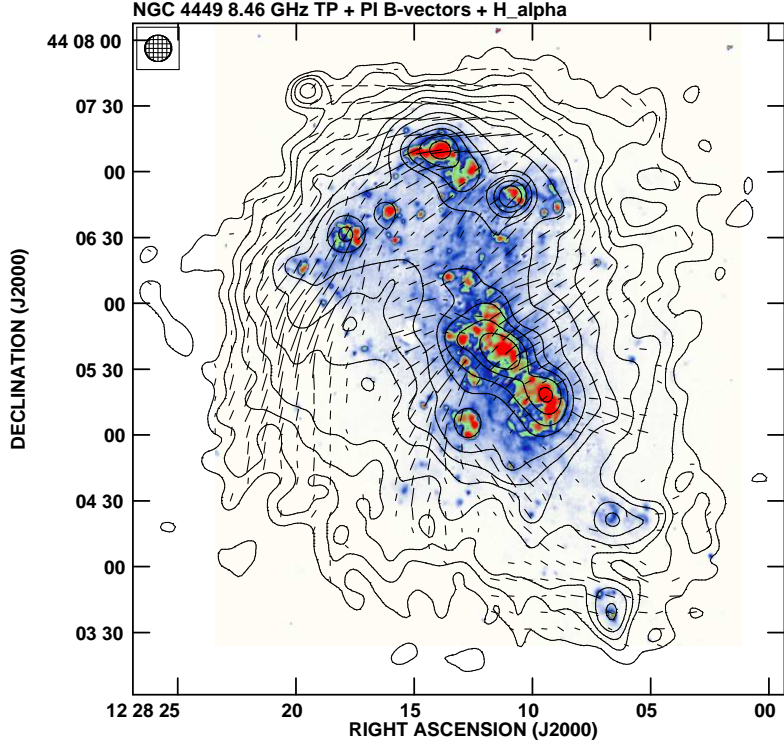


Figure 19: Contours of total radio emission and  $B$ -vectors of the Magellanic-type galaxy NGC 4449 at 8.4 GHz and  $12''$  resolution, combined from VLA and Effelsberg observations, overlaid onto an image of the  $H\alpha$  emission. Vector lengths are proportional to the polarized intensity (from Chyży et al. 2000).

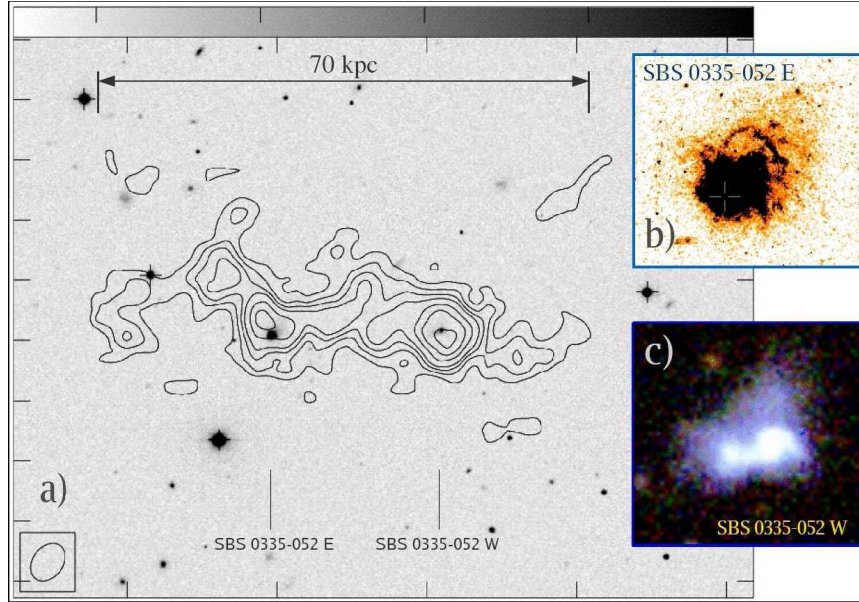


Figure 20: **a**: Optical image of the nearby ( $D=54$  Mpc) XBCD pair SBS 0335-052 E ( $Z_{\odot}/41$ ) and SBS 0335-052 W ( $Z_{\odot}/60$ ) with overlaid VLA HI contours (from Pustilnik et al. 2001). The XBCDs are immersed within a large, slowly rotating gas cloud with a projected size of  $\sim 70 \times 20$  kpc and a total HI mass of  $\sim 2 \times 10^9 M_{\odot}$ . **b** & **c**: HST and ESO NTT exposures of SBS 0335-052 E and SBS 0335-052 W (from Papaderos et al., in prep.).

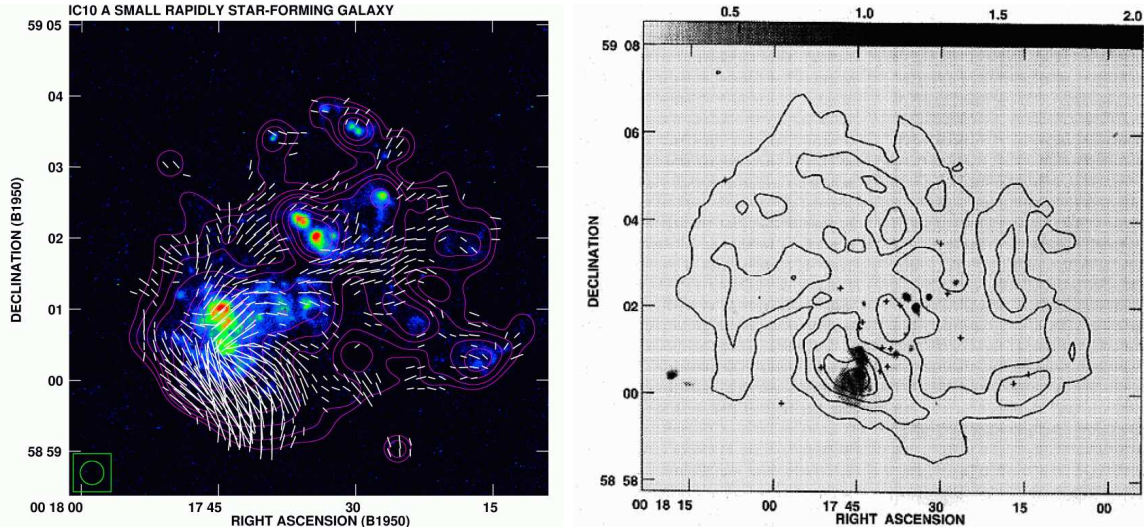


Figure 21: Left: Contours of total radio emission and  $B$ -vectors of the dwarf galaxy IC 10 at 4.8 GHz and  $20''$  resolution, observed with the VLA, with vector lengths are proportional to the polarized intensity (from Chyży et al. in prep.), overlaid onto an image of the H $\alpha$  emission by D. Bomans (see Chyży et al. 2003). Right: HI emission (contours) overlaid onto the radio continuum emission at 1.4 GHz (greyscale, from Yang & Skillman 1993).

some information on the proper motion of dwarf galaxies having undergone star formation over the past  $10^9$  yr.

The relativistic particles streaming into the halos of dwarf galaxies lose their energy on a time scale of  $\sim 10^8$  yr via synchrotron and inverse Compton radiation (Sect. 2.1). Although invisible at cm wavelengths, they could be still detectable at meter waves where their expected lifetime is 5 to 10 times longer. Assuming the aging relativistic particles travel at the Alfvénic speed in a magnetic field of  $B \simeq 1 \mu\text{G}$  with a thermal ion density of about  $0.001 \text{ cm}^{-3}$ , we can estimate that the relativistic particles visible at 120 MHz could move out to 30–40 kpc within 500 Myr or even further (say 60–80 kpc) when observed at lower frequencies. They should be detected at the  $5\text{-}\sigma$  level (0.5 mJy/b.a.) at 120 MHz in about 1 hour (with a synthesized beam of  $1''$ , i.e. with long baselines). LOFAR can easily resolve low-frequency halos of dwarf galaxies out to  $\sim 100$  Mpc, i.e. to Coma Cluster distances.

The ratio of high-frequency to low-frequency radiation may also provide a powerful tool to diagnose the star-forming history of dwarf galaxies. BCDs undergoing a post-starburst phase will easily be identifiable by their weak or absent radio emission at cm wavelengths while having still bright radio halos at meter wavelengths. By contrast, non-starburst, late-type DGs maintaining a nearly constant SFR over a long time will develop, just like late-type spirals, a characteristic cm/m flux ratio  $\epsilon$  only somewhat smaller than 1. If the standard dI $\Rightarrow$ BCD evolutionary scenario is correct, then LOFAR will discover a large population of quiescent dIs with a very small value of  $\epsilon$ . Conversely, if these two dwarf galaxy classes are not evolutionary related, larger flux ratios are to be expected for the majority of dIs. Such a test with LOFAR will place strong observational constraints on contemporary theories of dwarf galaxy evolution.

Substantial, partly ordered magnetic fields are found in optically small galaxies (dwarfs and low-surface brightness galaxies, LSBs) with rather disorderly velocity fields (Fig. 21, Chyży et al. 2003, 2007). Weakly ordered motions in their star-forming regions constitute a challenge to the standard mean-field dynamo mechanism (Sect. 4.1) requiring a long-time stable rotation. On the other hand, many dwarf irregulars possess a huge (tens of kpc) HI

halo rotating differentially in an ordered manner at speeds up to 80–100 km/s, resembling dynamically the disks of spiral galaxies (Bajaja et al. 1994, see another example in Fig. 20). The question of whether these halos may actively generate large-scale ordered magnetic fields remains open. Using LOFAR for a deep search for polarized low-frequency radio emission and/or Faraday rotation of distant polarized sources shining through the HI halo, together with deep H $\alpha$  imaging, will constrain magnetic field generation mechanisms. In particular, we can distinguish between the dynamo driven by cosmic rays (Hanasz et al. 2004) acting in star-forming places, and that driven by the magneto-rotational instability (Dziourkevitch et al. 2004), which is also present in a “quiet” (non star-forming) gas.

As the best objects we plan to observe:

- NGC 4449 — a dwarf galaxy known to have a large radio halo and quite strong and orderly magnetic fields (Klein et al. 1996, Chyży et al. 2000). The galaxy also has a very extended HI halo (Bajaja et al. 1994).
- NGC 1569 — a starburst dwarf galaxy with a large-scale HI structure, a HI companion and a so-called HI bridge to the east of the galaxy (Mühle et al. 2005). They also report low-intensity HI halo emission.

## 7 Giant radio galaxies

Giant radio galaxies (GRGs), defined as objects with dimensions larger than about 1 Mpc (assuming  $H_0=50$  km/s/Mpc and  $q_0=0.5$ ), are the largest single objects in the Universe (see e.g. Mack et al. 1998, Schoenmakers et al. 2000a, Machalski & Jamrozy 2006). Their large sizes are probably due to a combination of large age, powerful high-velocity jets and low density environments. Approximately 150 GRGs are known in the literature and among them is the largest object known, J1420-0545, with a projected linear size of about 6 Mpc (Machalski et al. 2008).

GRGs are extremely useful for studying a number of astrophysical problems. These range from understanding the evolution of radio sources, constraining the orientation-dependent unified scheme, to probing the intergalactic and intercluster medium at different redshifts. Spectral aging effects are best studied at the higher frequencies, while low-frequency observations can help to answer the question about the shape of the source spectra in the regime beyond which presently instruments cannot reach ( $\nu \leq 150$  MHz). Whether the spectra are still straight or bend towards low frequencies remains unknown, but this is important to estimate the injection spectral index and energy losses. Recent observations suggest that around at least some GRGs extended diffuse cocoons occur (Fig. 22). They provide important clues about the structure and the evolution of these sources. Neglecting the presence of those cocoons can cause serious under- or over-estimations of various physical parameters of radio galaxies, such as their entire volume, total luminosity, etc. Since such halos are thought to have low surface brightness, steep synchrotron spectra and large extents on the sky they are invisible from present-day investigations due to the existing observational limitations. With the superb resolution of LOFAR at low frequencies, detailed studies of giants at high redshift will become possible. These could be used to probe the intergalactic medium, i.e. its density and magnetic field.

Because of the low density in and around these giant sources, with lobes located far outside the gaseous spheres of the parent galaxies, GRGs can be expected to be highly polarized, even

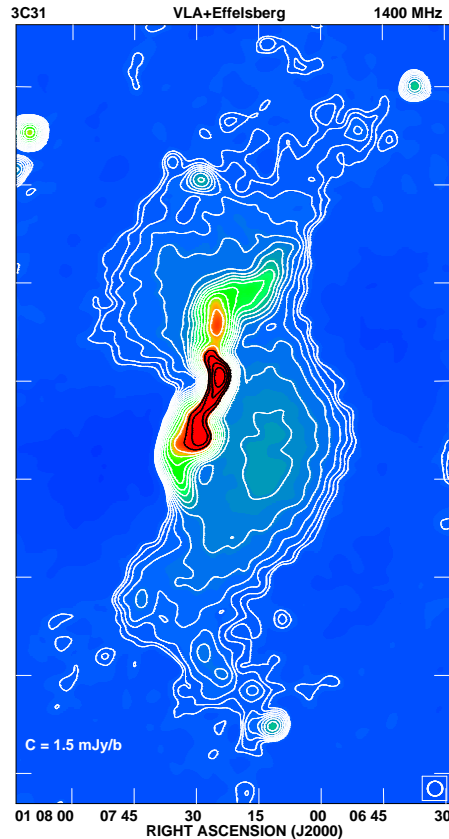


Figure 22: Giant radio galaxy 3C31 at 1.4 GHz from combined VLA NVSS and Effelsberg data (both contours and colors). The extended diffuse cocoon is well visible here (from Weżgowiec et al., in prep).

at low frequencies. This was indeed found to be the case (e.g. Strom & Jägers 1988, Mack et al. 1997). By studying the spatial distribution of the depolarization we can determine the Faraday depth of the emitting regions and thus constrain both the electron density and magnetic field strength inside and outside the lobes. Faraday depolarization of the emission from the two jets is known to be asymmetric (the *Laing-Garrington effect*, Garrington et al. 1988) and hence must occur in an extended halo acting as a foreground screen. This effect should be more prominent at low frequencies, and weak fields and low densities can be probed. The derived magnetic field strengths can be compared with those from equipartition and Inverse Compton emission arguments. To reduce beam depolarization by RM gradients will require high resolution and hence the long European baselines of LOFAR.

Among the class of giant radio galaxies there is a sub-group that is known as *double-double radio galaxies* (DDRGs: Schoenmakers et al. 2000b). Approximately a dozen or so DDRGs are known in the literature (Saikia et al. 2006). The explanation behind their morphology is that nuclear activity was temporarily switched off, thereby disrupting the flow of particles to the hot spot. When the activity is resumed, new channels are created and a new set of hotspots will develop. This model (Kaiser et al. 2000) requires that the inner lobes/hotspots form inside lower density regions. Again, radio polarimetry could help to constrain the viable models.

The polarized lobes are located in the intergalactic medium, possibly even in cosmic voids, so that they are ideal probes of the intergalactic magnetic field. A statistical investigation of a large sample with known redshifts is required.

## 8 Stellar and AGN jets

Accretion and mass ejection are among the most fundamental processes in the Universe. Accretion of matter onto compact, rotating, magnetized bodies is known to produce highly collimated, bipolar outflows of matter (“jets”) along the rotational axis of the central body. Such highly collimated outflows are ubiquitous in the Universe; they are found in a range of cosmic objects including our own Sun, brown dwarfs, planetary nebulae, protostars, young stellar objects (YSO), X-ray binaries, and galactic nuclei. This impressive variety covers a mass range extending over ten orders of magnitude, from  $\sim 0.1 M_{\odot}$  to  $\gtrsim 10^9 M_{\odot}$ . In all of these objects, collimated outflows transport excess angular momentum and energy from the vicinity of compact, rotating objects.

Details of the mechanism for extraction and transport of the energy and angular momentum may vary depending on the type of objects producing the outflows, but the underlying picture is similar in all types of the collimated outflows. Efficiency and magnitude of the energy extraction depend likely on the depth of the gravitational potential well and the electromagnetic fields of the central object. This results in a wide range of energy vested into outflows, depending on the type and physical conditions of different central objects. This underlines the specific importance of studies of collimated outflows in different types of astrophysical objects and across a large range of physical conditions. Such a multi-faceted approach is necessary for constructing a synthetic and fundamental picture of the accretion-ejection process.

Radio observations at low frequencies are particularly well-suited for addressing a wide range of problems related to collimated outflows that cannot be investigated in other bands of the electromagnetic spectrum. Low frequency observations will provide a unique tool for probing non-thermal synchrotron emission produced by the low energy tail of the plasma in the outer layers of the outflows and in the regions with highly evolved plasma such as extended lobes, relics and cavities produced by the jet activity in the interstellar and intergalactic medium. This information is crucial for studies of structure, formation and evolution of collimated outflows from Galactic and extragalactic objects. It will bring new dimensions to studies of the structure and dynamics of the outflows and allow us to perform detailed investigations of their interaction with the external medium. This will provide an outstanding foundation for detailed quantitative studies of evolution and re-acceleration of non-thermal plasma in cosmic objects. Measurements of polarization will give reliable estimates of the magnetic field distribution in the outflows, enabling investigations of the role it plays on extended scales, in Galactic and extragalactic objects. Low frequency studies of extragalactic jets will provide essential clues for understanding the power and efficiency of the kinetic feedback from AGNs and study the activity cycles in galaxies.

There are several major areas of astrophysical research in which the low-frequency information provided by observations with LOFAR is expected to produce a fundamental impact:

1. *Formation and evolution of collimated outflows from galactic and extragalactic objects.* LOFAR brings new dimensions to studies of the structure and dynamics of the outflows and allows detailed investigations of their interaction with the external medium to be made. For this purpose, it will be helpful to observe outflows in different environments. For example, comparison of AGN jets in dense cluster core regions with ones in less dense environments can tell us how such interactions contribute in regulating the outflow.

2. *Evolution of astrophysical plasmas.* Jet studies with LOFAR will provide an outstanding foundation for detailed quantitative studies of evolution and re-acceleration of non-thermal plasma in cosmic objects. Measurements of polarization will give reliable estimates of the magnetic field distribution in the outflows, enabling investigations of the role it plays

on extended scales, in galactic and extragalactic objects. In the case of strong nearby radio galaxies, additional Faraday rotation studies can yield further insight into the magnetic field distribution in the jets and their surrounding medium.

3. *AGN feedback and its impact on the Universe at large.* Studies of extragalactic flows at low frequencies will provide essential clues for understanding the power and efficiency of the kinetic feedback from AGNs and their effect on activity cycles in galaxies and cosmological growth of super-massive black holes. Such studies are critically needed for making a detailed assessment of the role played by AGNs in the formation and evolution of large-scale structures in the Universe.

4. *Evolution of nuclear activity in galaxies.* LOFAR observations will provide unsurpassed capabilities for detecting and studying the relics of galactic activity. This will enable a uniquely detailed account of activity cycles and long-term evolution of active galaxies to be made.

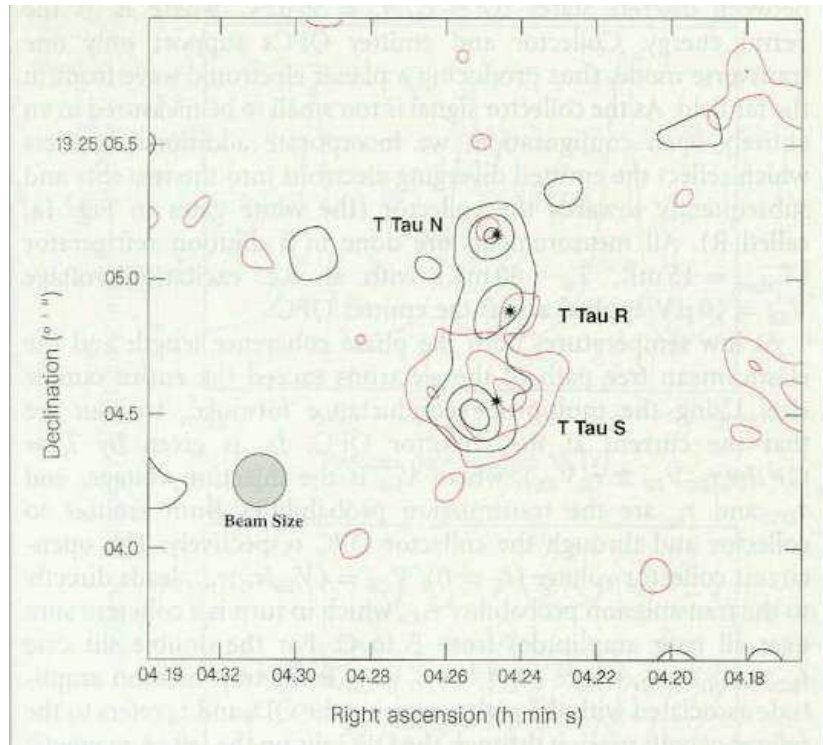


Figure 23: Left-handed (black) and right-handed (red) circular polarization observed with Merlin in the vicinity of the T Tau multiple system. Lobes of opposite polarization are seen centered on T Tau S, indicating opposite helicity of the magnetic field in the bipolar jet from this young star (from Ray et al. 1997).

One group of jet sources will be discussed now in more detail – jets from young stars are one of the most striking manifestations of star formation (Bally et al. 2007, Ray et al. 2007). This phenomenon has been studied over the past two decades, and there is general agreement that such jets are produced as a necessary consequence of the accretion of matter onto forming stars. This accreted matter would possibly dump its angular momentum onto the young stellar object, thereby spinning it up to break-up velocity in a short time. Jets seem to solve this so-called “angular momentum problem of star formation” by carrying the excess angular momentum away. The generally suggested mechanism for this process and the launching and collimation of jets is through “rotating magnetospheres” (Königl 1989,

Camenzind 1990). Field lines penetrating the accretion disk get wound up by the disks Keplerian rotation, thereby forming a paraboloidic structure. Ionized matter injected at its bottom (from the disk or star) will follow these wound-up field lines and get accelerated and collimated.

Among the jet sources, young stars may be the sources best suited to study the launching and collimation mechanism of jets in detail, since they are our closest jet sources, and thus allow us observations at the smallest absolute scales. In the nearest star forming regions, like Taurus, they are only about 140 pc away. In fact, young stars are the only jet sources that allow us to resolve the launching region spatially.

Recent observations from the ground with adaptive optics and with the Hubble Space Telescope (HST) have confirmed the paraboloid shape of the jet collimation region, and provide evidence for the rotation of stellar jets, as predicted by the rotating magnetosphere models (Bacciotti et al. 2002, Coffey et al. 2004, Woitas et al. 2005). The crucial test of these models is the detection of the magnetic field, and the measurement of its field strength and geometry. Such measurements are not feasible with, for example, Zeeman splitting of the atomic or molecular lines of the shock-excited gas in the jets seen from the ultraviolet to the infrared part of the spectrum, because of the small field strength. The only way to measure the magnetic fields is through synchrotron and gyro-synchrotron radiation in the radio regime.

Such measurements have been attempted at cm-wavelengths with the VLA and Merlin. While thermal emission could be observed in several jets, the non-thermal emission turns out to be at the very limits of sensitivity of these instruments – synchrotron radiation has been observed in two jets with the VLA (Curiel et al. 1993), while gyro-synchrotron radiation was observed in the outflow from the prototype young star T Tauri with Merlin while it was in a prolonged phase of outburst, and thus much brighter than usual (Fig. 23, Ray et al. 1997).

Calculations show that observations observations of the non-thermal emission in jets from young stars at meter wavelengths will be perfectly feasible with LOFAR. LOFARs spatial resolution will even allow us to resolve structure in this emission and measure it with distance from the source. Thus, LOFAR will allow us to confirm the magnetic fields in jets and measure them in detail. In this way, it will put our understanding of the accretion/ejection process in astrophysics on firm grounds. In the longer term, even studies of the variability, of the motion of the jet flow and the field in it may become possible.

We plan to do observations (including linear and circular polarization) of the  $\simeq 5$  best cases from a list of the closest sources of young stellar jets and sources for which radio emission has already been observed, respectively:

HH211, CW Tau, RY Tau, T Tau, FS Tau B, DG Tau B, DG Tau, HH30, HL Tau, DO Tau, RW Aur, HH34, HH212, HH26, HH72, Ser FIRS1, LkH $\alpha$ 233.

## 9 Intergalactic magnetic fields

The prediction of a large-scale cosmic web is one of the defining characteristics of large-scale structure simulations. Moreover, galaxies and the intra-cluster medium account for only approximately one third of the baryon density in the local Universe expected in a concordance cosmology. The majority of the missing baryons are likely to reside in a warm-hot intergalactic medium (WHIM) which in turn is expected to reside in the cosmic web of the large-scale structure. If the cosmic web also contains a magnetic field we can hope to detect this field

(and ultimately map the cosmic web) by either direct observation of synchrotron emission or Faraday rotation against background sources. Detection of this field, or placing stringent upper limits on it, will provide powerful observational constraints on the origin of cosmic magnetism.

Various mechanisms have been suggested for the origin of a magnetic field in the cosmic web. One possibility is that the fields are truly primordial, i.e. that a seed field formed prior to recombination (e.g. Banerjee & Jedamzik 2003). Alternatively, the field could be produced via the Weibel instability — small-scale plasma instabilities at structure formation shocks (Medvedev et al. 2004). A third possibility is that the field is injected into the WHIM via the action of injection from galactic black holes (AGNs) and other outflows (e.g. Kronberg 2004). In each case the field is subsequently amplified by compression and large-scale shear-flows (Brüggen et al. 2005, Dolag et al. 2002). Recently, Ryu et al. (2008) have argued that highly efficient amplification is possible via MHD turbulence, with the source of the turbulent energy being the structure formation shocks themselves (Fig. 24). Estimates of the strength of the turbulent field in filaments obtained from MHD simulations with a primordial seed field range typically between  $0.1 \mu\text{G}$  and  $0.01 \mu\text{G}$ , while regular fields are weaker.

From simulations it is expected that the strength of magnetic fields amplified by MHD turbulence in evolved galaxy clusters is mainly independent of the seed mechanism, since turbulent amplification is an efficient process and saturation is likely to have occurred in these objects. In the filamentary structures of the cosmic web, however, this is not the case. Cosmic-web filaments are hence anticipated to be far more sensitive to the origin of the seed fields. In particular, the extent of magnetic field penetration and its strength in filaments are expected to be much lower in the case that the origin of the field is from “late” astrophysical sources instead of a primordial one. As mentioned above, late sources with the ability to seed fields are active galactic nuclei or galactic winds. Primordial magnetic fields have been seeded prior to galaxy formation. For example, they could have been generated in the very early Universe, i.e. before recombination, and might have left a measurable imprint in the Cosmic Microwave Background. In conclusion, observations of cosmic magnetism in the low-density filamentary cosmic web are extremely useful for inferring the field origin.

With LOFAR it will be possible to search for synchrotron radiation from the cosmic web at the lowest possible levels. Its detection will probe the existence of magnetic fields in rarefied regions of the intergalactic medium, measure their intensity and possibly their polarization, and investigate their origin and their relation to the large-scale structure formation in the Universe. Possible evidence for magnetic fields associated with a filamentary cosmic web has been found in the cluster ZwCl 2341.1+0000 at  $z \sim 0.3$  (Bagchi et al. 2002) – the radio emission spans several Mpc following the filamentary network of galaxies. Recently, Brown & Rudnick (2009) reported similar filamentary emission in 0809+39 which is also highly polarized. In the latter case the emission was detected above  $3 \text{ mJy/beam}$  at  $327 \text{ MHz}$  using the WSRT.

Faraday rotation is a more sensitive tool to detect weak magnetic fields than synchrotron emission. Xu et al. (2006) found an excess of rotation measures (RM) towards two super-clusters which may indicate regular magnetic fields of  $< 0.3 \mu\text{G}$  on scales of order 500 kpc. Lee et al. (2009) found evidence for a  $30 \text{ nG}$  intergalactic field with about 1 Mpc coherence length, from a statistical correlation at the  $4\sigma$  level of the RMs of background sources with the galaxy density field.

LOFAR may measure magnetic fields in the cosmic web for the first time. For fields of  $\sim 10^{-8} - 10^{-9} \text{ G}$  along filaments of 10 Mpc length with electron density  $n_e \approx 10^{-5} \text{ cm}^{-3}$  (Kronberg 2006), Faraday rotation measures of between  $0.1$  and  $1 \text{ rad m}^{-2}$  are expected. A  $30 \text{ nG}$  regular field on a scale of 1 Mpc as claimed by Lee et al. (2009) would generate

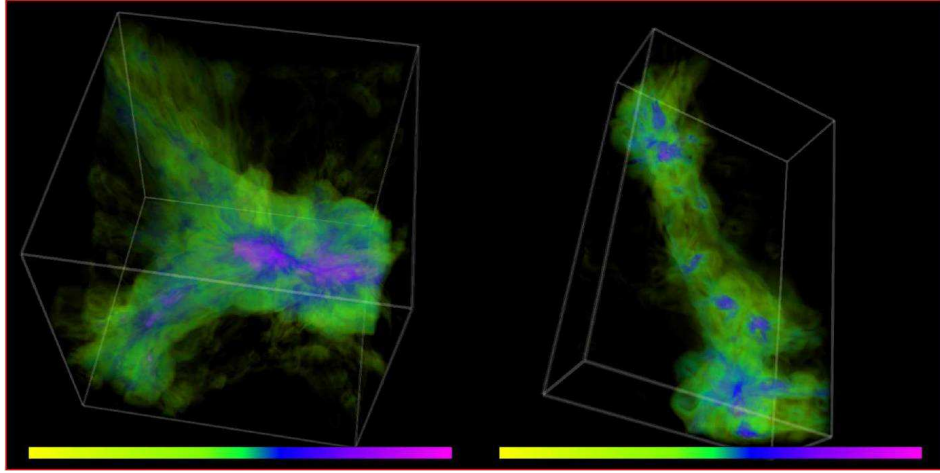


Figure 24: Simulation of magnetic fields in the Cosmic Web (at  $z = 0$ ) in a volume of  $25 h^{-1} \text{ Mpc}^3$  centered around a cluster complex (left panel) and in a volume of  $25 \times 15.6 \times 6.25 h^{-1} \text{ Mpc}^3$  which includes a number of galaxy groups along a filament (right panel). The colour codes the magnetic field strength (logarithmically scaled) from 0.1 nG (yellow) to  $10 \mu\text{G}$  (magenta). Clusters and groups are shown with magenta and blue, while filaments are green (from Ryu et al. 2008).

about  $0.2 \text{ rad m}^{-2}$ , which is similar to the expected RM accuracy of LOFAR and hence probably cannot be detected directly (see Sect. 10.1). Promising is a statistical analysis like the measurement of the power-spectrum of the magnetic field of the cosmic web (Kolatt 1998) or the cross-correlation with other large-scale structure indicators like the galaxy density field (Lee et al. 2009).

Apart from Galactic Faraday foregrounds, systematics due to source-intrinsic Faraday screens or of surrounding media in the direct neighborhoods of the sources can give rise to further contamination. In general, Faraday projection effects due to multiple traversed foreground screens may play an important role. It is very likely that prior information is required for disentangling contributions of different screens successfully via Faraday tomography. Moreover, background sources at medium to high redshifts are likely to have their polarized emission traversing several cosmic web filamentary structures which as well affects the obtained RM power spectrum. Redshift determination of polarized background sources might be necessary. How likely polarized light of a radio source at a given redshift traverses foreground screens also depends on the cosmology of the Universe. Therefore, the RM power spectrum depends on astrophysics and cosmology. However, given the specifications of LOFAR one might still stand a chance to statistically detect magnetic fields in the cosmic web and even analyze its structure. LOFAR's abilities given its wide frequency span, high resolution and high sensitivity are unique in this respect.

In addition to studying these weak intercluster magnetic fields, the RMs of cluster sources, large-scale structure filaments and background radio sources will also constrain the distribution and density of thermal gas at the interface of clusters and the cosmic web. Most of the ionized baryons in the Universe are believed to reside in intergalactic space at temperatures too low ( $\sim 10^6 \text{ K}$ ) to be detectable via X-ray emission (Cen & Ostriker 1999). RM measurements may then be our only hope to constrain the properties of this very important component of the Universe.

## 10 Observing program

### 10.1 Deep mapping and RM grids

The core part of the Magnetism Key Science Project (MKSP) is to deeply map the **diffuse total and polarized emission and its RM distribution** from selected regions in the Milky Way, a variety of nearby galaxies, galaxy groups, galaxies of the Virgo cluster and dwarf galaxies, as explained in detail in Sections 3–6. Diffuse *total* emission from extended disks and halos around nearby galaxies is best detected at low resolutions of  $10''$ – $60''$  (Dutch baselines only). The detection of diffuse *polarized* emission will not be possible from the star-forming inner disks due to Faraday depolarization, but instead from the outer disks and halos where Faraday effects are much weaker. High resolution may be needed to avoid beam depolarization, to be smoothed to lower resolution after RM Synthesis to detect the weak diffuse emission. The main depolarization effect is probably RM gradients. Because we aim for galaxies with diameters of several arcminutes, depolarization by internal RM gradients within the sources is more severe than by RM gradients in the Galactic foreground. To resolve the internal RM gradients in nearby galaxies, we may need angular resolutions of better than  $10''$ . The brightest nearby galaxies will allow polarization mapping with the international baselines at a resolution of  $\sim 1''$ .

Measuring the **RMs of a grid towards polarized background sources** behind the galaxies is a more sensitive way to detect weak regular fields because the signal-to-noise ratios are much higher than that of the diffuse galactic emission. Furthermore, depolarization by RM gradients in the foreground source is less severe as long as the angular extent of the background source is smaller than the beamsize. To achieve this, we need high a resolution of  $\sim 1''$ . A minimum of about 10 background sources is needed to recognize simple large-scale field patterns (Stepanov et al. 2008).

RM grids of polarized background sources towards selected galaxies and galaxy groups planned by the MKSP are an ideal precursor of the SKA Key Science Project *The origin and evolution of cosmic magnetism* which plans to perform an all-sky survey of Faraday rotation measures (RM) of compact extragalactic sources at 1.4 GHz, to model the three-dimensional structure and strength of the magnetic fields in the intergalactic medium and the interstellar medium of intervening galaxies and of the Milky Way (Gaensler et al. 2004). RM values from  $(1\text{--}5)\cdot 10^7$  polarized background sources with an accuracy of about  $\pm 5 \text{ rad m}^{-2}$  are expected (Beck & Gaensler 2004). This will allow the recognition of the dominant large-scale magnetic field structure in about 60,000 galaxies out to distances of 100 Mpc, to fully reconstruct the detailed magnetic field structure in nearby galaxies out to 10 Mpc (Stepanov et al. 2008), and to map the Milky Way magnetic field in unprecedented detail. An RM survey at the same frequency but with lower sensitivity is also planned for the Australian SKA precursor telescope ASKAP (project POSSUM).

The MKSP will develop the analysis tools needed for the future ASKAP and SKA surveys. Although fewer polarized sources are expected at lower frequencies, LOFAR can detect much smaller rotation measures down to about  $0.5 \text{ rad m}^{-2}$  (see below), thus becoming the telescope to measure the weakest cosmic magnetic fields so far.

The RM contribution from the Galactic foreground in the Galactic plane will be much larger than the RMs from galaxy halos, clusters and the IGM. In the 1.4 GHz DRAO/ATCA polarization survey of the Galactic plane ( $1'$  resolution), RMs of background sources of several  $100 \text{ rad m}^{-2}$  were observed (Brown et al. 2003, Haverkorn et al. 2006). RM gradients or fluctuations in the Galactic foreground can be several  $100 \text{ rad m}^{-2}$  for the average source separation of about one degree, which could cause strong depolarization at low frequencies within a large beam. In the 340–375 MHz WSRT polarization survey ( $5'$  resolution) of two

fields near the plane in the second Galactic quadrant the source density and RMs are lower ( $|RM| \leq 50 \text{ rad m}^{-2}$ ) (Haverkorn et al. 2003), probably due to depolarization effects within the large WSRT beam. Though RMs are much smaller at high Galactic latitudes (de Bruyn et al. 2006), Faraday depolarization in the Galactic foreground could still be a problem for the LOFAR RM survey. Simulations of the diffuse polarized Galactic foreground emission at arcsec angular resolution including small-scale magnetic field fluctuations with a Kolmogorov-like power law were recently made by Sun & Reich (2009), which will help in planning sensitive polarization LOFAR observations.

To avoid depolarization and reach the best possible RM sensitivity, RM gradients have to be resolved to better than  $0.1 \text{ rad m}^{-2}$  per beam which may need about  $1''$  resolution and hence require the international LOFAR with maximum baselines of about 400 km.

To avoid significant bandwidth depolarization, the spectral resolution has to be  $\delta\nu/\text{kHz} \leq 1.7 \cdot 10^4/|RM|$  at 120 MHz which will be achievable with LOFAR even for large  $|RM|$ . The spectral resolution of the raw LOFAR visibilities is 0.7 kHz. Even at a frequency of 50 MHz the maximum detectable  $|RM|$  for 0.7 kHz channels is still  $1200 \text{ rad m}^{-2}$ .

*RM Synthesis* (see Sect. 2.3) applied on LOFAR's large number of channels can trace almost the whole range of expected RM values and separate the RM components from distinct foreground and background regions (Brentjens & de Bruyn 2005). The total range  $\Delta\lambda^2$  in  $\lambda^2$  space determines the RM resolution  $\delta\phi$ . The channel width  $\delta\lambda^2$  determines the maximum observable Faraday depth  $\phi_{max}$  (see Fig. 1).  $\lambda_{min}^2$  determines the maximum scale in Faraday depth  $L_{\phi,max}$  of a region at which total back-to front depolarization is reached. A region with a scale in Faraday depth below  $L_{\phi,max}$  is called *Faraday-thin*.

Within polarized background sources (which we expect to be mostly distant double or extended radio galaxies), Faraday depolarization can occur by RM gradients along the jets, lobes and bridges as well as beam depolarization due to different polarization angles in unresolved jets. To resolve a jet of 1 kpc length at 100 Mpc distance, a resolution of  $1''$  is needed, requiring international baselines of  $\simeq 400 \text{ km}$  at 200 MHz. With this resolution and LOFAR's excellent sensitivity, a very large number density of polarized background sources can be expected. As soon as some LOFAR baselines between 50–100 and 250 km (Exloo–Effelsberg) become available we plan to conduct test observations to ascertain the beam depolarization effects in extragalactic (double) radio sources.

In a survey with the Dutch LOFAR array (36 stations) which is limited by confusion in total intensity, the total number of sources with total flux densities above  $5\times$  the rms noise within LOFAR's primary beam is  $\simeq 2 \cdot 10^5$ , almost independent of frequency (see Table 11 of the LOFAR Survey Specifications, Version 2.2). Assuming that the distribution of the polarization fractions is Gaussian, centered on  $p \simeq 3\%$ , as in the NVSS at 1.4 GHz (Beck & Gaensler 2004), we expect several thousand polarized sources within the primary beam. This estimate may be too pessimistic because the mean degree of polarization at 1.4 GHz increases to about 5% towards lower flux densities (Taylor et al. 2007). On the other hand, the majority of the sources at the relevant flux densities (about 0.3–1 mJy at 200 MHz) are expected to be starburst galaxies which may well be unpolarized at low frequencies due to Faraday depolarization.

At 200 MHz the mean angular distance between polarized sources will be about  $1'$  (optimistic case) and  $3'$  (pessimistic case), which is sufficient to map the RM distribution in nearby galaxies and clusters. The required  $1-\sigma$  noise level with the Dutch LOFAR corresponding to the confusion level in total intensity is about  $20 \mu\text{Jy}$  at 200 MHz,  $40 \mu\text{Jy}$  at 150 MHz,  $60 \mu\text{Jy}$  at 120 MHz and  $300 \mu\text{Jy}$  at 60 MHz (see Survey Specifications document of the Surveys KSP). To reach the confusion level with a total bandwidth of 32 MHz, about 2000 hours of integration time are needed at 200 MHz, about 300 hours at 150 MHz, about 200 hours at

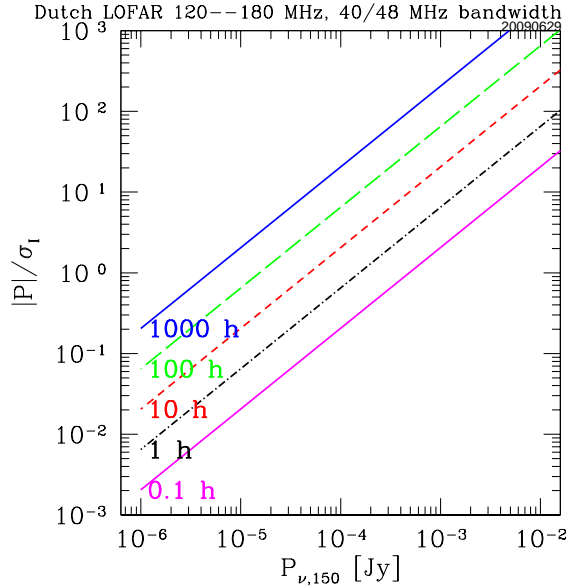


Figure 25: Observation time needed to reach a certain signal-to-noise ratio  $Q_p = P/\sigma$  for observations at  $45^\circ$  elevation, spanning the 120–180 MHz band, and assuming an effective total bandwidth of 40 MHz and the Dutch LOFAR array of 36 stations.

120 MHz and about 2500 hours at 60 MHz. The confusion level for polarization is at least  $10\times$  lower than that for total emission.

Fig. 25 shows the required observation time to reach a certain signal-to-noise ratio in the 120–180 MHz band. We wish to reach an rms noise level of  $15 \mu\text{Jy}$  at 150 MHz with the Dutch array (36 stations) and  $10 \mu\text{Jy}$  with the international array (44 stations) which needs about 100 hours of integration per field with the maximum available bandwidth of 40 MHz (reserving 8 MHz for the simultaneous observation of calibration fields).

The RM error (the resolution in FD space) is  $\delta\phi \approx \sqrt{3}/(Q_p \Delta\lambda^2)$ . To achieve  $\delta\phi = 0.1 \text{ rad m}^{-2}$  in the highband, covering the maximum frequency span of 120–240 MHz, we need a signal-to-noise ratio  $Q_p$  of the polarized emission of  $\simeq 4$ . If the frequency span is only 120–150 MHz, we need  $Q_p \simeq 8$ . Fig. 26 gives the required observation time to reach a certain RM error  $\delta\phi$  in the 120–180 MHz band. Within 100 hours we will reach an rms noise of  $15 \mu\text{Jy}$  and  $\delta\phi \simeq 0.1 \text{ rad m}^{-2}$  for sources with  $75 \mu\text{Jy}$  polarized flux density.

Observations in the lowband can in principle yield very small RM errors (see Fig. 2 in Sect. 2.3). Spanning the 60–80 MHz frequency band,  $Q_p \simeq 2$  would already be sufficient to reach this accuracy. However, polarization and RM observations in the lowband are much more difficult than in the highband and will critically depend on the achievable accuracy of polarization and ionospheric calibration (see Sects. 10.2 and 10.3).

The MKSP plans to observe the following objects and fields. Precise frequency ranges and subband settings are still to be worked out in detail during the commissioning phase. They depend among other things on RFI and RM Synthesis optimization.

- **Commissioning phase:**

Find polarized calibrators, test instrumental and ionospheric calibration, test RM Synthesis and RM Cleaning, optimize frequency settings, search for polarization in the lowband, test wide-field calibration, test deep integration, measure number density of polarized background sources. Commissioning proposals have been submitted for the 30 Sept 2009 deadline.

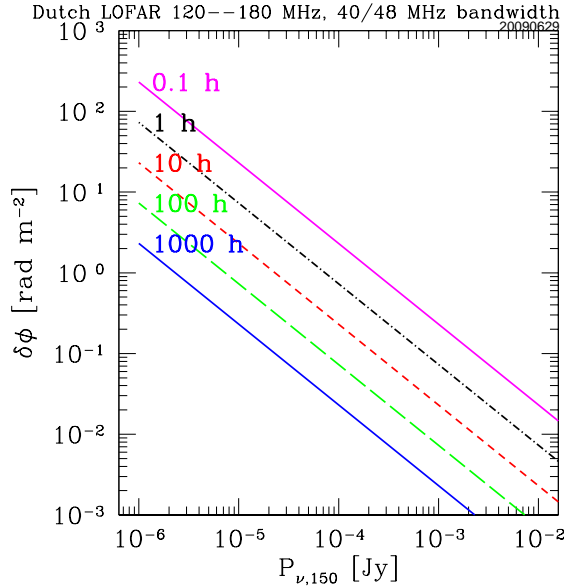


Figure 26: Observation time needed to reach a certain RM error  $\delta\phi$  for sources with a polarized flux density  $P$  detected at the  $5\sigma$  level, for observations at  $45^\circ$  elevation, spanning the 120–180 MHz band, and assuming an effective total bandwidth of 40 MHz and the Dutch LOFAR array of 36 stations.

- **All-sky surveys** (30–50, 60–80, 120–150, and 180–210 MHz) — piggyback with the Surveys KSP:  
Catalogue of polarized sources, test RM Synthesis, measure galaxy spectra and spectral curvatures, find polarized galaxies.
- **Milky Way:**  
We plan to “piggy-back” on all stages of the Survey KSP in order to learn about the largely unknown low-frequency polarized sky, for a further systematic approach of Galactic emission properties and their separation from deep extragalactic observations. For a proper analysis of the polarization data, large-scale emission components (to be observed with single-stations or a few LOFAR core stations) must be added, although small-scale Faraday effects will significantly reduce the maximum size of structures in Stokes U and Q compared to shorter wavelength. Narrow-band spectral analysis and RM Synthesis will then be used for an analysis of the emission components along the line of sight. These fields are to be specified from the survey data, however, some interesting areas are already identified by deep higher frequency observations aiming to study the CMB B-mode (e.g. Carretti et al. 2006). Other interesting fields are selected by a low column density of interstellar matter components (e.g. the Lockman Hole, minimum dust emission, minimum total intensity, etc.). These fields have the potential for particularly deep extragalactic observations and likely have a less complex Galactic foreground.
- **Survey of 60 nearby galaxies** spanning the 180–210 MHz band with 13 MHz total bandwidth and 9 h integration time per field, using 36 Dutch plus 8 international stations, giving about  $50 \mu\text{Jy}$  rms noise:  
Spectral index maps, search for thermal absorption, search for extended halos and polarized emission, RM Synthesis (spectra in FD space), find best cases for the deep fields.

The galaxy list has been prepared together with the Surveys KSP.

- **Polarization of 10 giant radio galaxies** in three frequency bands (50–70, 120–180 and 180–230 MHz) with total bandwidths of 16, 48 and 48 MHz, respectively, and 5 h integration time per source, using 36 + 8 stations, giving about 70  $\mu$ Jy rms noise in the highband:

Spectral index maps, RM Synthesis (FD spectra), depolarization and Laing-Garrington effect, probing the intergalactic medium around the lobes with RM (see Sect. 7).

- **Observations of 5 stellar jets** spanning the 120–180 MHz frequency band with 48 MHz total bandwidth and 20 h integration time per source, using 36 + 8 stations, giving about 35  $\mu$ Jy rms noise:

Search for non-thermal emission and its linear and circular polarization, and measure magnetic fields (see Sect. 8).

- **Deep mapping and RM grids:**

This is the heart of the Project. We plan to observe about 10 fields around nearby galaxies and galaxy groups. The final choice will depend on the results from the earlier surveys.

- Aims: deep mapping of the total and polarized diffuse emission and a grid of RM values from background sources, separation of Galactic and extragalactic components

- Targets: a few nearby galaxies (face-on and edge-on) (see Sect. 4.2) plus a few examples of other species (tidally interacting and gas-stripped galaxies, dwarf galaxies, strongly star-forming and LSB irregulars, and compact galaxy groups) (see Sects. 5–6).

The deep fields will be located at different Galactic latitudes and will also be analyzed with respect to the properties of the small-scale magnetic field in the foreground of the Milky Way, e.g. by computing the structure functions as a function of Galactic latitude.

- Requested resolutions: 1–10'' (diffuse emission),  $\approx 1''$  (grid)

- Frequency span: 120–180 MHz

- Total bandwidth: 48 MHz (of which 8 MHz are used for calibration)

- Requested noise level: 10  $\mu$ Jy rms noise

- Requested observation time per field: 100 h, assuming 36 + 8 stations

Lowband observations will follow if polarization and ionospheric calibration can be achieved with sufficient accuracy.

- Detecting RM signals from **intergalactic magnetic fields** (Sect. 9) is a challenge which requires a very large areal source density and hence a very high sensitivity. In addition we need a well-behaved Galactic foreground. Proof for an intergalactic origin of (part of) the RM could come from a statistical comparison with source redshift. The best candidates are deep fields around compact galaxy groups with minimum Galactic foreground contribution.

## 10.2 Polarization calibration

The calibration of a phased array like LOFAR requires a proper full polarization treatment of the signal and the instrument. The Measurement Equation (Hamaker et al. 1996) provides

the mathematical framework to describe and calibrate polarization effects. This would be required even if none of the celestial signals were intrinsically polarized at these frequencies. That is, the success of LOFAR depends on a proper treatment of instrumental polarization.

Fortunately, there are also intrinsically polarized signals at LOFAR frequencies. WSRT observations in the 1-meter (310–390 MHz) and 2-meter (115–180 MHz) bands already reveal highly polarized discrete (pulsars) and diffuse signals from the Milky Way. In addition to the instrumental polarization effects, we also have to worry about the ionosphere which is between LOFAR and the rest of the Universe.

The additional complexities introduced by polarization observations with LOFAR must not lead to delayed implementation, because for both the EoR and Magnetism KSP polarization calibration is crucial. Issues that will be given dedicated attention are:

- Construction of a grid of all-sky discrete polarized sources that can be used as polarization calibrators. Using long baselines, e.g. between the LOFAR core in Exloo and the Effelsberg LOFAR station, we will start a program to observe, at high angular resolution, extragalactic double radio sources that are known to be highly polarized at high frequencies ( $> 300$  MHz) .
- In addition to using discrete polarization calibrators, we will develop approaches to utilize patches of highly polarized Galactic foreground as calibrators, e.g. the “Fan” region as located with the WSRT in the LFFE band (Bernardi et al. 2009).
- We have to develop, test and learn all the tricks in the first few years of operation before we reach solar maximum, expected in 2013 (when Faraday rotation effects will become more complex). This means that preliminary reduction pipelines that include ionospheric Faraday rotation have to be in place as soon as possible.
- We expect to encounter position-dependent Faraday rotation even within a station beam. This has to be solved as an image-plane effect just like phase non-isoplanaticity.
- In order to image very local, hence very large angular scale, total intensity and polarization signals, we will require data on very short, intra-station, baselines. The time to experiment with this type of information is during the CS1 commissioning phase. Special attention will have to be paid to intra-station cross-talk.
- We have to develop procedures on how to deal with (eventually) missing short spacings in polarization self-calibration (Hamaker 2006).
- We have to develop procedures which utilize self-calibration phase information, as well as a minimum ionospheric model, to predict Faraday rotation.

### 10.3 Ionospheric calibration

The ionosphere has two major effects on low-frequency data: total phase delay and Faraday rotation of polarized signals. The total phase delay will (have to) be solved via self-calibration using a global sky model for the discrete source population. The Faraday rotation of the polarized signal will have to be corrected through a model for the electron distribution and the Earth’s magnetic field in the Faraday-active part of the ionosphere. The average  $|RM|$  of the ionosphere varies between 0 and about  $5 \text{ rad m}^{-2}$ , depending on time of day, season and solar cycle. Looking southward at  $30^\circ$  elevation during in the afternoon during solar maximum, it can be as large as  $80 \text{ rad m}^{-2}$ . However, it is the short-term temporal variations that we have to worry about. A change of  $0.1 \text{ rad m}^{-2}$  rotates the polarization angle by

200° at a frequency of 50 MHz causing complete cancelation of the polarization signal if not properly corrected for. Calibration of the ionosphere can be done in a number of ways: (1) via an electron density model constructed from GPS data (which are by orders of magnitude too coarse for LOFAR calibration, but valuable as a starting point for absolute ionospheric electron density measurements), (2) through polarized calibrators with stable polarization angle and RM, (3) by using global total delay data from the LOFAR phase self-calibration solutions. In practice we will use data from all three methods.

#### 10.4 Relations to the other LOFAR Key Science Projects

Several tasks of the MKSP will be performed in close collaboration with the Surveys KSP, which is reflected in several double memberships. The all-sky surveys will enable to measure number counts statistics of polarized sources down to sub-mJy total flux densities, to select the galaxy survey to be observed jointly, and to estimate the required integration time for the deep fields planned by the MKSP.

The windows to measure signals from the Epoch of Reionization (EoR) will be targeted on special areas in the Galactic halo with relatively little polarized foreground emission which would then be ideal targets for our deep polarization studies. Long spacings are required to measure and subtract the foreground. The properties of the Galactic foreground are one common interest between the Magnetism and the EoR KSPs. The extreme requirements on polarization calibration in our Magnetism KSP are shared by those of the EoR KSP. We expect a close collaboration especially during the commissioning phase of LOFAR. Several members of the EoR KSP have expertise in both research areas and are also members of the MKSP.

Two science areas will be exploited in collaboration with the Transients KSP: RMs from polarized pulsars, and jets of young stars and active galactic nuclei.

#### 10.5 Theoretical investigations

Accompanying theoretical work is planned supporting the analysis of the data gained by the MKSP. Synthetic RM data cubes computed for ISM models with different field structure are under development as a collaboration between MPIfR Bonn, MPA Garching, and NAOJ Beijing (coordinated by W. Reich, MPIfR). Improved dynamo models for the Milky Way and spiral galaxies are being developed in collaboration with groups in Torun, Newcastle, Manchester, Potsdam, Moscow, and Perm (coordinated by R. Beck, MPIfR). A joint German-Russian project on the evolution of magnetic fields in galaxies is funded by DFG and RFFI. There will be detailed simulations of the radio emission resulting from the large-scale structure formation, which will help to find and interpret intergalactic magnetic fields. The groups at Cambridge, JU Bremen and MPA Garching have demonstrated expertise in these areas. Two projects of the new Research Group funded by the German Research Foundation (DFG) are dedicated to simulations of galaxies and clusters. Furthermore, detailed investigations of algorithms for statistical signal extraction about magnetic fields and their turbulence from RM and synchrotron data sets will be performed. The groups at Bonn, Cambridge, Dwingeloo, Garching, and Kraków have gathered and demonstrated substantial experience in this field.

## References

- [1] Appleton, P. N., Xu, K. C., Reach, W., et al. 2006, *ApJ*, 639, L51
- [2] Armstrong, J. W., Rickett, B. J., & Spangler, S. R. 1995, *ApJ*, 443, 209
- [3] Arshakian, T. G., Beck, R., Krause, M., & Sokoloff, D. 2009, *A&A*, 494, 21
- [4] Bacciotti, F., Ray, T. P., Mundt, R., Eisloffel, J., & Solf, J. 2002, *ApJ*, 576, 222
- [5] Bagchi, J., Enßlin, T., Miniati, F., et al. 2002, *New Astr.*, 7, 249
- [6] Bajaja, E., Huchtmeier, W. K., & Klein, U. 1994, *A&A*, 285, 385
- [7] Bally, J., Reipurth, B., & Davis, C. J. 2007, in *Protostars and Planets V*, University of Arizona Press, p. 215
- [8] Banerjee, R., & Jedamzik, K. 2003, *Phys. Rev. Lett.*, 91, 251301
- [9] Beck, R. 2005, in *Cosmic Magnetic Fields*, eds. R. Wielebinski & R. Beck (Berlin: Springer), p. 41
- [10] Beck, R. 2006, *AN*, 327, 512
- [11] Beck, R. 2007, *A&A*, 470, 539
- [12] Beck, R. 2009, *Ap&SS*, 320, 77
- [13] Beck, R., & Gaensler, B. M. 2004, in *Science with the Square Kilometre Array*, eds. C. Carilli & S. Rawlings (Amsterdam: Elsevier), *New Astron. Rev.*, 48, 1289
- [14] Beck, R., & Krause, M. 2005, *AN*, 326, 414
- [15] Beck, R., Brandenburg, A., Moss, D., Shukurov, A., & Sokoloff, D. 1996, *Ann. Rev. A&A*, 34, 155
- [16] Beck, R., Fletcher, A., Shukurov, A., et al. 2005, *A&A*, 444, 739
- [17] Bernardi, G., de Bruyn, A. G., Brentjens, M. A., et al. 2009, *A&A*, 500, 965
- [18] Bertone, S., Vogt, C., & Enßlin, T. 2006, *A&A*, 370, 319
- [19] Bomans, D. J., van Eymeren, J., Dettmar, R.-J., Weis, K., & Hopp, U. 2007, *New Astron. Rev.*, 51, 141
- [20] Brandenburg, A., & Subramanian, K. 2005, *Phys. Rep.*, 417, 1
- [21] Brandenburg, A., Donner, K. J., Moss, D., et al. 1992, *A&A*, 259, 453
- [22] Brentjens, M. A., & de Bruyn, A. G. 2005, *A&A*, 441, 1217
- [23] Brown, J. C., Taylor, A. R., & Jackel, B. J. 2003, *ApJS*, 145, 213
- [24] Brown, J. C., Haverkorn, M., Gaensler, B. M., et al. 2007, *ApJ*, 663, 258
- [25] Brown, S., & Rudnick, L. 2009, *ApJ*, 137, 3158
- [26] Brüggén, M., Ruszkowski, M., Simionescu, A., Hoeft, M., & Dalla Vecchia, C. 2005, *ApJ*, 631, L21

- [27] Camenzind, M. 1990, *Rev. Mod. Astron.*, 3, 234
- [28] Carretti, E., Poppi, S., Reich, W., et al. 2006, *MNRAS*, 367, 132
- [29] Cen, R., & Ostriker, J. P. 1999, *ApJ*, 514, 1
- [30] Chung, A., van Gorkom, J. H., Kenney, J. D. P., & Vollmer, B. 2007, *ApJ*, 659, L115
- [31] Chyży, K. T., & Beck, R. 2004, *A&A*, 417, 541
- [32] Chyży, K. T., Beck, R., Kohle, S., et al. 2000, *A&A*, 356, 757
- [33] Chyży, K. T., Knapik, J., Bomans, D. J., et al. 2003, *A&A*, 405, 513
- [34] Chyży, K. T., Soida, M., Bomans, D. J., et al. 2006, *A&A*, 447, 465
- [35] Chyży, K. T., Bomans, D. J., Krause, M., et al. 2007, *A&A*, 462, 933
- [36] Clegg, A. W., Cordes, J. M., Simonetti, J. M., & Kulkarni, S. R. 1992, *ApJ*, 386, 143
- [37] Clemens, M. S., Alexander, P., & Green, D. A. 1998, *MNRAS*, 297, 1015
- [38] Coffey, D., Bacciotti, F., Woitas, J., Ray, T. P., & Eisloffel, J. 2004, *ApJ*, 604, 758
- [39] Condon, J. J., Helou, G., Sanders, D. B., & Soifer, B. T. 1993, *AJ*, 105, 1730
- [40] Condon, J. J., Helou, G., & Jarrett, T. H. 2002, *AJ*, 123, 1881
- [41] Curiel, S., Rodriguez, L. F., Moran, J. M., & Canto, J. 1993, *ApJ*, 415, 191
- [42] de Bruyn, A. G., Katgert, P., Haverkorn, M., & Schnitzeler, D. H. F. M. 2006, *AN*, 327, 487
- [43] Dolag, K., Bartelman, M., & Lesch, H. 2002, *A&A*, 387, 383
- [44] Duncan, A. R., Reich, P., Reich, W., & Fürst, E. 1999, *A&A*, 350, 447
- [45] Dziourkevitch, N., Elstner, D., & Rüdiger, G. 2004, *A&A*, 423, L29
- [46] Elmegreen, B. G., & Scalo, J. 2004, *ARAA*, 42, 211
- [47] Ferrière, K. M., & Schmitt, D. 2000, *A&A*, 358, 125
- [48] Frisch, P. C. 1998, *Space Sci. Rev.*, 86, 107
- [49] Gaensler, B. M., Beck, R., & Feretti, L. 2004, in *Science with the Square Kilometre Array*, eds. C. Carilli & S. Rawlings (Amsterdam: Elsevier), *New Astron. Rev.*, 48, 1003
- [50] Gaensler, B. M., Haverkorn, M., Staveley-Smith, L., et al. 2005a, in *The Magnetized Plasma in Galaxy Evolution*, eds. K. Chyży, K. Otmianowska-Mazur, M. Soida, & R.-J. Dettmar, p. 209
- [51] Gaensler, B. M., Haverkorn, M., Staveley-Smith, L., et al. 2005b, *Science*, 307, 1610
- [52] Gao, Y., Zhu, M., & Seaquist, E. R. 2003, *AJ*, 126, 2171
- [53] Garrington, S. T., Leahy, J. P., Conway, R. G., & Laing, R. A. 1988, *Nat*, 331, 147
- [54] Gastaldello, F., Buote, D. A., Humphrey, P. J. et al. 2007, *ApJ*, 669, 158

- [55] Gray, A. D., Landecker, T. L., Dewdney, P. E., & Taylor, A. R. 1998, *Nat*, 393, 660
- [56] Hamaker, J. P. 2006, *A&A*, 456, 395
- [57] Hamaker, J. P., Bregman, J. D., & Sault, R. J. 1996, *A&AS*, 117, 137
- [58] Han, J. L., Beck, R., & Berkhuijsen, E. M. 1998, *A&A*, 335, 1117
- [59] Hanasz, M., Kowal, G., Otmianowska-Mazur, K., & Lesch, H. 2004, *ApJ*, 605, L33
- [60] Haverkorn, M., Katgert, P., & de Bruyn, A. G. 2003, *A&A*, 403, 1031, and *A&A*, 403, 1045
- [61] Haverkorn, M., Katgert, P., & de Bruyn, A. G. 2004, *A&A*, 427, 169, and *A&A*, 427, 549
- [62] Haverkorn, M., Gaensler, B. M., Brown, J. C., et al. 2006, *AN*, 327, 483
- [63] Haynes, M. P., Giovanelli, R., & Roberts, M. S. 1979, *ApJ*, 229, 83
- [64] Heald, G. 2009, LOFAR Magnetism KSP Memo No. 1
- [65] Heald, G., Braun, R., & Edmonds, R. 2009, *A&A*, 503, 409
- [66] Heesen, V., Beck, R., Krause, M., & Dettmar, R.-J. 2009a, *A&A*, 494, 563
- [67] Heesen, V., Krause, M., Beck, R., & Dettmar, R.-J. 2009b, *A&A*, 506, 1123
- [68] Hummel, E., & Dettmar, R.-J. 1990, *A&A*, 236, 33
- [69] Kaiser, C. R., Schoenmakers, A. P., & Röttgering, H. J. A. 2000, *MNRAS*, 315, 381
- [70] Kenney, J. D. P., Tal, T., Crowl, H. H., Feldmeier, J., Jacoby, G. H. 2008, *ApJ*, 687, L69
- [71] Kepley, A. A., Mühle, S., Everett, J., et al. 2009, *AJ*, in prep.
- [72] Klein, U., Weiland, H., Brinks, E. 1991, *A&A*, 246, 323
- [73] Klein, U., Haynes, R.F., Wielebinski, R., & Meinert, D. 1993, *A&A*, 271, 402
- [74] Klein, U., Hummel, E., Bomans, D. J., & Hopp, U. 1996, *A&A*, 313, 396
- [75] Königl, A. 1989, *ApJ*, 342, 208
- [76] Kolatt, T. 1998, *ApJ*, 495, 564
- [77] Krause, M. 2003, in *The Magnetized Interstellar Medium*, eds. B. Uyaniker et al. (Katlenburg: Copernicus), p. 173
- [78] Krause, M. 2009, *Rev. Mex. AyA*, 36, 25
- [79] Kronberg, P. P. 2002, *Physics Today*, 55, 120000
- [80] Kronberg, P. P. 2003, *Physics of Plasmas*, 10, 1985
- [81] Kronberg, P. P. 2006, *AN*, 327, 517
- [82] Kronberg, P. P., Lesch, H., & Hopp, U. 1999, *ApJ*, 511, 56
- [83] Lee, J., Pen, U.-L., Taylor, A. R., Stil, J. M., & Sunstrum, C. 2009, arXiv:0906.1631

- [84] Machalski, J., & Jamrozy, M. 2006, A&A, 454, 95
- [85] Machalski, J., Koziel-Wierzbowska, D., Jamrozy, M., & Saikia, D. J. 2008, ApJ, 679, 149
- [86] Mack, K.-H., Klein, U., O’Dea, C. P., & Willis, A. G. 1997, A&AS, 123, 423
- [87] Mack, K.-H., Klein, U., O’Dea, C. P., Willis, A. G., & Saripalli, L. 1998, A&A, 329, 431
- [88] Macquart, J.-P., & de Bruyn, A. G. 2007, MNRAS, 380, L20
- [89] Martin, C. L. 1998, ApJ, 506, 222
- [90] Medvedev, M. V., Silva, L. O., Fiore, M., Fonseca, R. A., & Mori, W. B. 2004, JKAS, 37, 533
- [91] Minchin, R., Davies, J., Disney, M., et al. 2007, ApJ, 670, 1056
- [92] Minter, A. H., & Spangler, S. R. 1996, ApJ, 458, 194
- [93] Mühle, S., Klein, U., Wilcots, E. M., & Hüttemeister, S. 2005, AJ, 130, 524
- [94] Noutsos, A., de Bruyn, A. G., & Stappers, B. W. 2009, LOFAR Magnetism KSP Memo No. 2
- [95] Patrikeev, I., Fletcher, A., Stepanov, R., et al. 2006, A&A, 458, 441
- [96] Pen, U.-L., Chang, T.-C., Hirata, C. M., et al. 2008, arXiv0807.1056
- [97] Peterson, J. D., & Webber, W. R. 2002, ApJ, 575, 217
- [98] Phookun, B., & Mundy, L. G. 1995, ApJ, 453, 154
- [99] Pustilnik, S., Brinks, E., Thuan, T. X., et al. 2001, AJ, 121, 1413
- [100] Ray, T. P., Dougados, C., Bacciotti, F., Eisloffel, J., & Chrysostomou, A. 2007, in *Protostars and Planets V*, University of Arizona Press, p. 231
- [101] Ray, T. P., Muxlow, T. W. B., Axon, D. J., et al. 1997, Nat, 385, 415
- [102] Redfield, S., & Linsky, J. L. 2008, ApJ, 673, 283
- [103] Reich, W. 2006, in *Cosmic Polarization 2006*, ed. R. Fabbri (Kerala: Research Signpost), p. 91, astro-ph/0603465
- [104] Reynolds, R. 2004, Adv. Space Res., 34, 27
- [105] Ryu, D., Kang, H., Cho, J., & Das, S. 2008, Science, 320, 909
- [106] Saikia, D. J., Konar, C., & Kulkarni, V. K. 2006, MNRAS, 366, 1391
- [107] Schekochihin, A. A., Cowley, S. C., Taylor, S. F., Maron, J. L., & McWilliams, J. C. 2004, Ap&SS, 292, 141
- [108] Schnitzeler, D. H. F. M., Katgert, P., Haverkorn, M., & de Bruyn, A. G. 2007, A&A, 461, 963
- [109] Schoenmakers, A. P., Mack, K.-H., de Bruyn, A. G., Röttgering, H. J. A., Klein, U., & van der Laan, H. 2000a, A&AS, 146, 293

- [110] Schoenmakers, A. P., de Bruyn, A. G., Röttgering, H. J. A., van der Laan, H., & Kaiser, C. R. 2000b, MNRAS, 315, 371
- [111] Siemieniec-Ozieblo, G., & Ostrowski, M. 2000, A&A, 355, 51
- [112] Skillman, E. D., & Klein, U. 1988, A&A, 199, 61
- [113] Soida, M., Urbanik, M., Beck, R., Wielebinski, R., & Balkowski, C. 2001, A&A, 378, 40
- [114] Soida, M., Beck, R., Urbanik, M., & Braine, J. 2002, A&A, 394, 47
- [115] Spoelstra, T. A. T. 1984, A&A, 135, 238
- [116] Stepanov, R., Arshakian, T. G., Beck, R., Frick, P., & Krause, M. 2008, A&A, 480, 45
- [117] Stil, J., Krause, M., Beck, R., & Taylor, R. 2009, ApJ, 693, 1392
- [118] Strickland, D. K., Heckman, T. M., Colbert, E. J. M., et al. 2004, ApJ, 606, 829
- [119] Strom, R. G., & Jägers, W. J. 1988, A&A, 194, 79
- [120] Sun, X. H., & Reich, W. 2009, A&A, 507, 1087
- [121] Sun, X. H., Han, J. L., Reich, W., et al. 2007, A&A, 463, 993
- [122] Sun, X. H., Reich, W., Waelkens, A., & Enßlin, T. A. 2008, A&A, 477, 573
- [123] Taylor, A. R., Stil, J. M., Grant, J. K., et al. 2007, ApJ, 666, 201
- [124] Testori, J. C., Reich, P., & Reich, W. 2008, A&A, 484, 733
- [125] Trinchieri, G., Sulentic, J., Pietsch, W., & Breitschwerdt, D. 2005, A&A, 444, 697
- [126] Tüllmann, R., Dettmar, R.-J., Soida, M., Urbanik, M., & Rossa, J. 2000, A&A, 364, L36
- [127] Urbanik, M. 2005, in *The Magnetized Plasma in Galaxy Evolution*, eds. K. Chyży, K. Otmianowska-Mazur, M. Soida, & R.-J. Dettmar, p. 201
- [128] Vollmer, B., Balkowski, C., Cayatte, V., van Driel, W., & Huchtmeier, W. 2004a, A&A, 419, 35
- [129] Vollmer, B., Beck, R., Kenney, J. D. P., & van Gorkum, J. H. 2004b, AJ, 127, 3375
- [130] Vollmer, B., Soida, M., Beck, R., et al. 2007, A&A, 464, L37
- [131] Vollmer, B., Soida, M., Chung, A., et al. 2008, A&A, 483, 89
- [132] Weżgowiec, M., Urbanik, M., Vollmer, B., et al. 2007, A&A, 471, 93
- [133] Whiting, C. A., Spangler, S. R., Ingleby, L. D., & Haffner, L. M. 2009, ApJ, 694, 1452
- [134] Widrow, L. M. 2002, RMP, 74, 775
- [135] Wieringa, M. H., de Bruyn, A. G., Jansen, D., Brouw, W. N., & Katgert, P. 1993, A&A, 268, 215
- [136] Williams, B. A., Yun, M. S., & Verdes-Montenegro, L. 2002, AJ, 123, 2417

- [137] Woitas, J., Bacciotti, F., Ray, T. P., Marconi, A., Coffey, D., & Eisloffel, J. 2005, *A&A*, 432, 149
- [138] Wolleben, M., & Reich, W. 2004, *A&A*, 427, 537
- [139] Wolleben, M., Landecker, T. L., Reich, W., & Wielebinski, R. 2006, *A&A*, 448, 411
- [140] Xu, C. K., Lu, N., Condon, J. J., Dopita, M., & Tuffs, R. J. 2003, *ApJ*, 595, 665
- [141] Xu, Y., Kronberg, P. P., Habib, S., & Dufton, Q. W. 2006, *ApJ*, 637, 19
- [142] Yang, H., & Skillman, E. D. 1993, *AJ*, 106, 1448
- [143] Zhu, M., Gao, Y., Seaquist, E. R., & Dunne, L. 2007, *AJ*, 134, 118